A Vibrotactile Display Design, evaluation and Fabrication

by

Ehsan Masnavi

A thesis
presented to the University of Waterloo
in fulfillment of the
thesis requirement for the degree of
Master of Applied Science
in
Systems Design Engineering

Waterloo, Ontario, Canada, 2011

AUTHOR'S DECLARATION

I hereby declare that I am the first and main author of this thesis. This is a true copy of the thesis, including any required final revisions, as accepted by my examiners. Chapter Two, Chapter Four and Chapter Five of this thesis were edited and revised by Wayne Giang, Catherine Burns and John S. Zelek.

Chapter Two and Chapter Five of this thesis were first written for a Defence Research and Development Canada (DRDC) report to support the Joint Unmanned Aerial Vehicle Surveillance Target Acquisition System (JUSTAS) project. These materials were prepared under a government of Canada contract and are under crown copyright.

I understand that my thesis may be made electronically available to the public.

Abstract

Vision and audition are the two best understood modalities which humans use to interact with the outside world. These modalities can provide highly precise spatial and temporal information. Thus, the field of human-computer interface design has focused much of their study and design on these modalities. On the other hand, the sense of touch has been largely ignored despite the fact that it is an essential part of human ability to interact with the environment.

We are interested to identify key findings on how to use tactile technology effectively to design and fabricate a tactile interface. We intend to design a wearable tactile interface which can assist Unmanned Aerial Vehicles (UAV) operators in supervisory control and monitoring tasks.

Tactile displays are usually comprised of vibratory stimulators which are arranged in specific formation based on the application of the display. Quantitative properties of a vibrating tactor which was used as the vibratory stimulator in our tactile interface were investigated and evaluated in this study. We executed a series of experiments to investigate the intensity of vibrations that the vibrating tactor can generate when it is being activated through different electrical signals. Driving signals were different in terms of waveform, frequency and amplitude.

By applying the outcomes of our experiments, and using the available guidelines for the design of tactile displays, we proposed some methods for displaying flight dynamics (Roll, Pitch and Yaw) of a UAV through a tactile display which is structured in form of a vest. Due to the relative infancy of this branch of information presentation, and also the lack of thorough discussion within the scientific community we need to execute further experiments to evaluate the performance of the suggested tactile display.

Acknowledgements

I am indebted to numerous people without whom my Masters studies would have been a much harder and less fruitful experience, and to only few of them I can give a particular mention here.

I had the privilege to be supervised by Professor John S. Zelek who offered me his assistance and unequivocal support in all possible fashions. I would like to express my sincere gratitude for his valuable guidance.

Professor Catherine Burns is especially thanked for supporting me during my Masters studies. I would like to express my sincere gratitude for her valuable guidance, critical advice and patience and for being a great academic role model. Many thanks are extended to professors Hamid Tizhoosh for reading my thesis and for providing helpful and insightful comments.

I owe thanks to the Department of Systems Design Engineering for offering all the necessary amenities and facilities. Particularly, I am very grateful for the Lab Instructor Tariq Naqvi for all his indispensable efforts and his readiness to help at all times.

Words fail me to express my heartfelt gratitude for my parents who, through my childhood and study career, provided me with all their love and encouragement and worked hard to secure me an excellent education. I regret that I would never be able to pay them back. I wholeheartedly thank Mahnaz Masnavi, Atefeh Masnavi and Alireza Masnavi for being a true sisters and brother and for being there for me whenever I needed help.

My friends at AIDL lab, Wayne Giang and Plinio Morita are especially thanked for being very supportive colleagues during my Masters studies.

Amin Safaei is especially thanked for being a true brother and helping and supporting me during my Bachelors and Masters studies.

Last but not least, I convey special acknowledgement to my friends, Maral Hamedani, Seyed Mostafa Shameli, Darioush Ghaffari Tari, Soroush Omidvar and Jonathan Gagne who made my stay in Waterloo enjoyable and made me feel at home. I also highly value the friendship of Adel Fakih and his support during my Masters studies and for being the perfect lab mate.

Dedication

To my parents, Asadollah Masnavi and Behjat Hezary.

Table of Contents

List of Figures

List of Tables

Chapter 1

Introduction

Vision and audition are the two best understood modalities which humans use to interact with the outside world. These modalities can provide highly precise spatial and temporal information. Thus, research in human-computer interface design and human factors engineering has focused on these modalities [1], [2]. On the other hand, the sense of touch has been largely ignored despite the fact that it is an essential part of human ability to interact with the environment. In the last few years, there has been a very rapid growth of interest in the development and application of interfaces which utilize tactile technology as a way of communicating spatial and navigation information to operators [2], [3], [4], [5], [6], [7], [8]. Therefore, the possibility of using the body surface as a communication medium now appears to be more possible than ever before.

In this thesis we are interested to identify key findings on how to use tactile technology effectively to design and fabricate a wearable tactile interface which can assist UAV operators in supervisory control and monitoring tasks. UAVs are remotely piloted aircraft used for a variety of civilian and military applications. They do not carry human operator and can be remotely controlled. Therefore, they can effectively reduce life risk, weight and fuel consumption in operations [9]. There has been increased development and application of UAVs in military and civilian forces.

In terms of controllability, UAVs come in two major types: some are controlled manually from a remote location, and others fly autonomously based on pre-determined flight plans using more complex automation systems. UAVs that are manually controlled from remote locations suffer from decreased operator performance due to loss of necessary sensory cues. As an example, it is difficult for an operator to scan the visual environment surrounding a UAV which is flown miles away from the control station. Also delays in control and communication systems make it difficult to precisely control these kinds of UAVs. In contrast, for autonomous UAVs the human factors issues are primarily related to issues with supervisory control such as problems in monitoring, decision making, and situation awareness.

Autonomous UAV systems consist of an autonomous aerial vehicle and a Ground Control Station (GCS). Many current GCS units require the use of an operator who is responsible for monitoring and supervisory control tasks. For instance, operators may be needed to delay or cancel certain critical

1

events such as landing or take-off during an operation [9]. Many of the supervisory tasks can be enhanced through the use of a tactile interface.

The objective of this thesis is to design and evaluate a wearable vibrotactile interface which can assist UAV operators in control and monitoring tasks. The interface includes a tactor vest comprised of vibratory stimulators. The stimulators are miniature vibrators which can be arranged in specific formation based on the type of information that is needed to be displayed. The tactor vest in worn by UAV operators and maps information regarding spatial orientation of an UAV to the skin of the torso.

1.1 Thesis Overview

This thesis is composed of three main sections:

1. Tactile Perception:

In this section we reviewed the current literature in tactile perception and analyzed available guidelines for the design of vibrotactile displays.This section examines how individuals perceive information in the tactile modality, with a focus on vibrotactile stimuli.

2. Electronic Hardware Design and Fabrication:

A vibrotactor display is comprised of vibratory stimulators which are arranged in a specific formation based on the application of the display. In order to produce different driving electrical signals for the vibrotactors which are used in the vibrotactor vest, we require a controller hardware. In this section we have provided descriptions about the design of a controller hardware which is used for activating vibrotactors.

3. Proposed methods for displaying spatial orientations through the tactor vest:

In this section we intend to provide some proposals regarding the presentation of the intensity of flight dynamics (roll, pitch and yaw) in a UAV through the tactor vest. We provide descriptions about our proposed methods and tactor configurations for several cases.

Chapter 2
Tactile Perception

2.1 Introduction

In this chapter we are interested in developing a strong foundation of tactile perception research because it can be a foundation for the effective use of vibrotactile displays. For this reason, we have started at an anatomical level. Subtle effects of tactor stimulation of the skin, such as adaptation rates and discrimination and localization ability, can have implications on how tactile displays should be designed. The review demonstrates that key findings from the basic science governing the sense of touch are relevant to interface design. This section also includes guidelines regarding vibrotactile parameters which can be used in generating tactile messages using a tactor vest.

This section is organized as follows:

Section 2.1. Provides an anatomical overview of human skin to provide insight into how tactors produce sensation. Section 2.2. Discusses the effects of vibrotactile stimuli placement, and localization issues on the torso. These effects are important in understanding how to design tactile signals in a vibrotactile display. Section 2.3. Describes the vibrotactile spatial acuity of the human torso and the effects of vibrotactile timing parameters on localization performance. This provides the foundation for the basic design of tactile signals for human worn devices. Section 2.4. Provides guidelines for coding information through vibrotactile displays. Section 2.5. Discusses different types of vibrotactile patterns along with a discussion of the research results. Section 2.6. Reviews other tactile characteristics. Section 2.7. Discusses the current understanding of masking effects in tactile displays. Section 2.8. Presents concluding remarks and summary of tactile perception.

This chapter of the thesis was first written for a Defence Research and Development Canada (DRDC) report to support the Joint Unmanned Aerial Vehicle Surveillance Target Acquisition System (JUSTAS) project [9]. These materials were prepared under a government of Canada contract and are under crown copyright.

3

2.2 Anatomic Overview of the Skin

We know from experience that a simple tap can immediately draw our attention. The nervous system is very capable of spatially localizing stimuli on the skin. For this reason, stimulation of the skin can be a powerful way to passively convey spatial information. The surface of the body might play an important role in presenting information to operators in situations where their other senses are being used or overloaded [2]. In the last few years, there has been rapid growing interest in the development and application of interfaces which use tactile technology as a way of communicating spatial and navigational information to operators [3], [2], [8].

The anatomical characteristics of human skin receptors have been discussed in detail in numerous reviews [10], [11], [12]. Only a brief summary is provided in this section in order to provide a basic understanding of how tactile displays influence the body. Skin is the largest receptive organ on the human body [13]. There are various receptor structures buried deep in the multi-layered tissue of the skin. In order to design applicable interfaces, the understanding of the various sensitivities of the skin's sensors and their responses to external stimuli is helpful. To date, the majority of studies of tactile interfaces have focused on mechano-receptors located within the glabrous (hairless) skin of the human. As Figure 1 depicts, underneath the surface of the glabrous skin, three thin layers exist: The first layer is the epidermis and its thickness varies from 0.4 mm to 1.6 mm. The second layer is the dermis which is about 6 times thicker than the epidermis and the third one is the subcutis (hypodermis) [1], [13].

The skin contains a variety of sensory organs called receptors. These are divided into four main groups by the type of stimuli that they are sensitive to: *mechanoreceptors* which are sensitive to pressure, vibration and slip, *thermoreceptors* which are sensitive to changes in temperature, *nocioreceptors* which are pain receptors, and *proprioceptors* which give information about the position of the limb in space. Various receptors respond to particular vibration frequencies and have different tendencies to adapt to vibratory stimuli. Frequency and adaptation characteristics should be considered in the design of tactile displays.

Referring to Figure 1, four kinds of mechanoreceptors lie in the skin tissue, each at specific depths of the skin [14], [15], [1]:

- *Meissner corpuscles* are a stack of nerve fibres, located in the grooved projections of the skin surface formed by epidermal ridges, situated perpendicular to the skin surface. They respond to light touch and are velocity sensitive. They are sensitive to vibrotactile stimuli in the range of 10

4

– 100Hz. They have highest sensitivity (lowest threshold) when sensing vibrations less than 50Hz. Meissner corpuscles are categorized as *rapid adapting* (RA) receptors which respond quickly to a stimulus, but rapidly adapt to it and stop responding when subjected to a constant stimulus.

- *Merkel receptors* are disk shaped receptors that respond to pressure and texture, but also to low frequency (5-15 Hz) vibratory input. They are categorized as *slow adapting* (SA) receptors which adapt slowly to stimulus and continue to transmit when subjected to constant pressure. Tactile display systems, by necessity, are in constant contact with the skin and are not well suited for the stimulation of SA type receptors.

- *Ruffini corpuscles* are spindle shaped receptors that respond to skin stretch and mechanical deformation within joints, specifically angle changes up to 2 degrees. They contribute to providing feedback for the grip and grasping function. These are categorized as SA receptors and are located in the deep layers of the skin.

- The *Pacinian corpuscles* are the largest receptors of the skin. These are located deeper in the skin and most susceptible to the vibrations in the 200-350 Hz frequency range. Pacinian corpuscles are categorized as RA receptors. This means that the effect of stimuli degrades rapidly after onset. Pacinian corpuscles discharge only once per stimulus application, hence they are not sensitive to steady pressure.

In general, the most effective and applicable receptors in tactile display applications are the Merkel cells for pressure sensation, the Meisner corpuscle for low frequency and the Pacinian corpuscle for high-frequency vibrations [13]. The most relevant receptors for the design of the tactile vest, which make use of C2 tactors operating at an optimal frequency of 250 Hz, are the Pacinian corpuscles**.**

2.3 The Effects of Placement on Vibrotactile Localization on the Torso

There have been several attempts since the 19th century to investigate the spatial acuity of the skin on several body parts. Generally, as we move from distal regions (such as the hands) to proximal regions (such as the torso) of the body, the sensitivity to stimuli degrades. The law of mobility states that the skin's sensitivity to locating and discriminating touched locations improves as the mobility of parts of the body increase [16], [17]. In addition to this, vibratory stimuli can be localized more effectively when they are located on anatomical points of reference. For example, when Cholewiak and Collins [18] evaluated vibratory stimuli localization at the various sites of the arm, they concluded that stimuli were localized

best when they were presented near the wrist, elbow, and shoulder. As a result, when developing tactile displays where spatial localization should be optimized, the design should consider taking advantage of anatomical points of reference to improve localization.
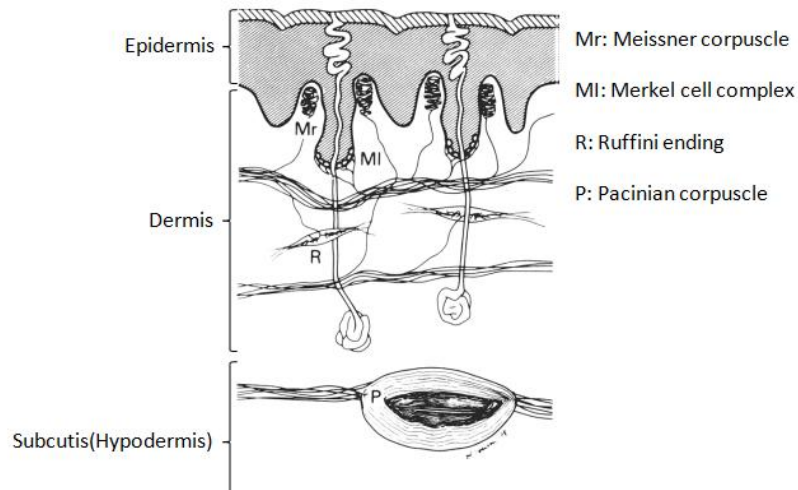
Figure 1: Glabrous skin anatomy. Picture taken from Lederman and Klatzky (p. 1440) [1]**.**

The majority of research that has attempted to investigate the accuracy and limitations of the sense of touch has typically tended to present stimuli to more sensitive regions of skin, such as the hands and finger tips [18], [19]. Although hands may have better discriminative power than the rest of the body, most current interfaces already require the use of the operator's hands and limbs for control activities. This fact highlights the importance of investigating the potential for using the surface of the torso as an alternative way to convey information. The three-dimensional nature of the body presents a natural mapping for three-dimensional spatial information [20]. Individuals tend to use the orientation of the trunk as a frame of reference in determining their self-orientation. This is because the head and limbs do not provide a stable frame of reference since they rotate relative to the trunk [21]. Therefore, knowing the effects of space and place on the vibrotactile localization on the torso is essential.

Several comprehensive experiments have been performed by Van Erp as well as Cholewiak and his colleagues. These researchers have investigated the ability for individuals to localize vibratory stimuli around the torso [16], [22]. Both of these experiments were conducted with the use of vibrotactors. Vibrations are commonly used as stimuli since the skin rapidly adapts to stationary touch and pressure

[23]. "Adaptation may be generally defined as a reduction in sensitivity resulting from a continuous unchanging stimulus" [14]. Therefore, taps on the skin have to be repeated in order to create a vibratory stimulus that the skin will not adapt to. In general, people can distinguish a temporal gap of 5 ms between successive taps on the skin [1]. Pressure based stimuli is more susceptible to adaptation, and is only sensitive to Merkel receptors. Vibrotactile stimuli on the other hand can be sensed by Pacinian corpuscles, the largest of the receptor structures in the skin. It is important to note that Cholewiak et al. [16] used the same C2 tactors which are used in our tactile vest.

2.3.1 Torso Location and Localization

Arrays of vibrotactors can be used to represent the location of an object relative to body in the environment. Cholewiak et al. [16], in the first part of their experiment, presented stimuli using vibrotactors situated at 12 equidistant locations on two belts. The belts encircled the abdomen and the lower margin of the rib. The reason for using two levels (abdomen and lower margin of the rib) was to see whether the characteristics of the underlying tissue would affect the localization of the vibrotactile stimuli. The vibrotactors located on the frontal side of the lower belt were placed on the tissue of the abdomen, whereas vibrotactors of the upper belt were over the ribs. In each trial, one stimulus (vibrotactor) was activated.

The first portion of the experiment revealed that the participant's performance in detecting stimuli around the abdomen and the rib cage was similar. Therefore for the torso, the underlying tissue type plays a minor role in vibrotactile spatial location. The ability to localize a stimulus around the torso was found to be a function of proximity to the spine (6 o'clock) and the navel (12 o'clock). It was found that observers were more capable of correctly detecting stimulus near the spine (6 o'clock) and the navel (12 o'clock) and these points can serve as anatomical reference points for the trunk. For this reason, in designing tactile displays, the spine and the navel can be used as reference locations in spatial tactile displays.

2.3.2 Tactor Separation and Localization

In the second part of the Cholewiak et al. [16] experiment, the number of vibrotactors on the belt was varied to evaluate whether better localization performance is possible with a decreased number of tactors. This was inspired by information transmitted and channel capacity of the observer notions described by Miller [24]. Arrays of 8 and 6 tactors were used as test conditions. The results of the second part of the experiment, compared against those obtained with the 12-tactor condition in the first part are shown in the polar plot presented in Figure 2. Overall performance around the torso was found to be dramatically

improved when the number of vibrotactors was reduced, though there was still variation in performance based on the location of the tactor.
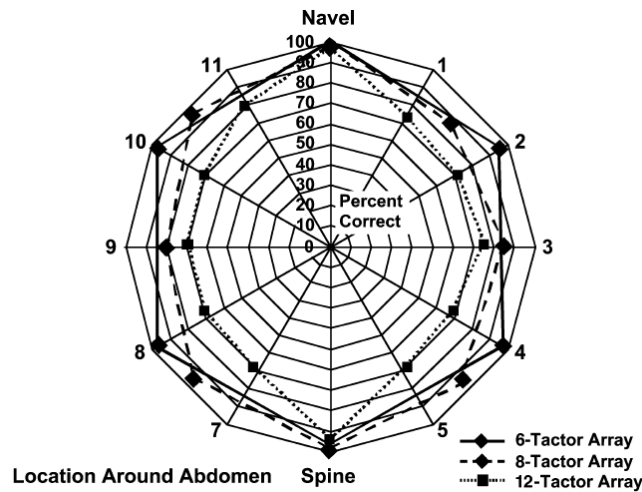
Figure 2: Localization performance around the abdomen for 6, 8, and 12 vibrotactile belts. Figure taken from Cholewiak et al. (p. 979) [25].

Similarly to the first part of the experiment, participants had the highest level of performance when localizing stimuli which were located at the navel and the spine when compared to other locations on the torso. This was true for the 6, 8, and 12 tactor array conditions. The results of this experiment suggest that increasing the separation between tactors and thus decreasing the number of vibratory stimuli improves the localization performance dramatically. In consideration of this, tactile pattern designs should take into consideration that increased tactor separation and reduced stimuli may improve localization performance. In order to demonstrate the importance of the spine and navel anchor points as points of reference, the vibrotactors belt arrays were rotated slightly so that tactors fell on the sides of these points. As shown in Figure **3**, in both these cases, the performance decreased.

In the third part of the experiment, 7 vibrotactors were located on a short strip spanning roughly half the circumference of the body and this tactor strip was used in 4 locations on the torso: front, back, left side and right side of the body. In the first case the array across the abdomen (front) was arranged so tactor 1 was at the left, tactor 4 at the navel and tactor 7 at the right side. For the back case, tactor 1 was at the right side, tactor 4 at the spine and tactor 7 at the left side of the body. The other two cases had similar

orientations, but had tactors that started at the navel or spine, and a center tactor (tactor 4) on either the left or right side of the body. The results of these experiments are depicted in Figure 4. Better performance was obtained when the tactor strip was used on the front and back, when compared to when it was located on the left side or right side of the body.

Summarizing the results of the Cholewiak et al. [16] experiments we can derive three main conclusions:

1- The spine and the navel can work as natural anchor points and observers are more capable of correctly detecting stimulus near these points.
2- Performance is found to be dependent on the number of tactors around the body, therefore increasing the separation among the tactors improves the localization ability.
3- Individuals are better able to localize tactors placed on the front and back of the torso than either the left or right sides of the body.
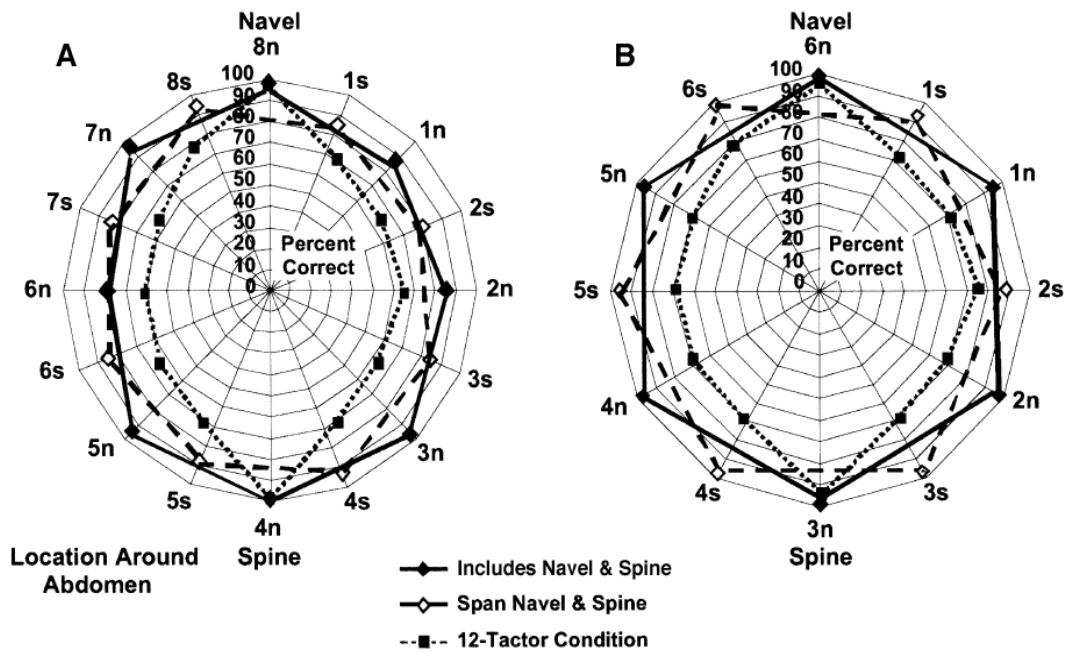
Figure 3: Localization performance around the abdomen; A) for 8 tactors and B) for 6 tactors. The solid lines in each graph connect the performances for the conditions that two of the tactors were situated on the spine and the navel (n); dashed lines connect the performances for the condition that the navel and the spine were

9

spanned (s). The data represented by the dotted lines are from the first part of the experiment (12 tactor condition). Figures taken from Cholewiak et al. (p. 980) [16]**.**
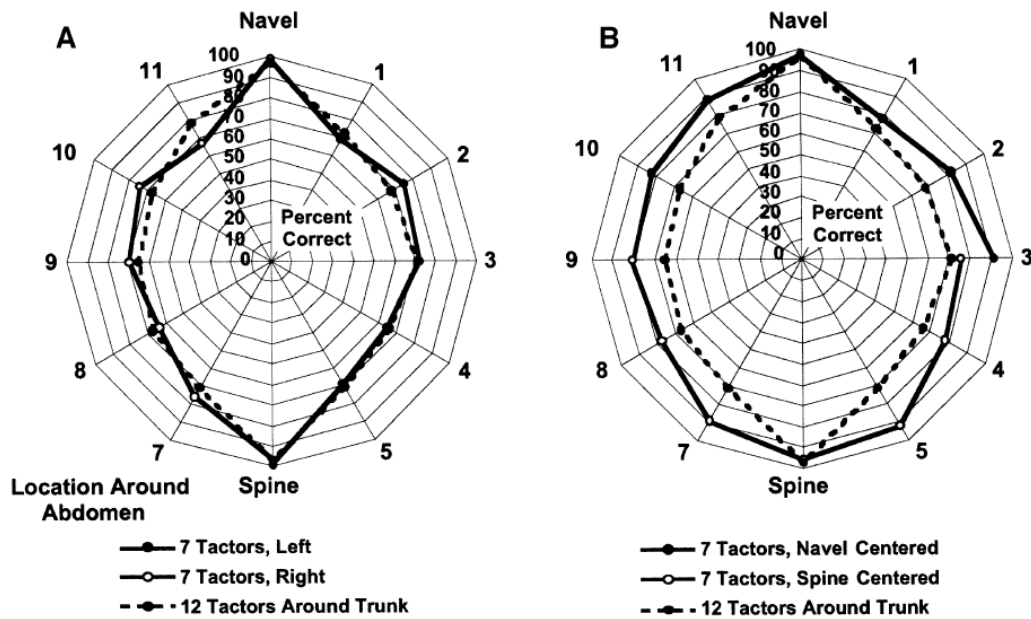
Figure 4: Localization performance for seven tactors presented to seven sites of the body in 4 cases. Figures taken from Cholewiak et al. [16] **(p. 983)**.

2.3.3 Origin of Reference Points for Tactor Localization

In another study by Van Erp[22], participants wore a tactor belt consisting of 15 vibrotactors. Tactors were embedded equidistantly around the belt's circumference. The middle tactor was located just above the navel. One stimulus, consisting of a vibrating tactor, was activated in each trial. The participants were asked to indicate the location of the vibration on a horizontally positioned square board, which they were seated within (by means of a specialized apparatus which was designed for this experiment).

Figure **5** shows the results of this experiment. Van Erp [22] found that there was a bias between the actual location of the tactors on the torso and the locations indicated by the participants as their response. The bias was toward the midsagittal plane, that is, perceived locations were located towards the navel for the tactors located on the abdomen and towards the spine for the tactors located on the back. This result is consistent with the findings of Cholewiak et al. [16] and supports the fact that the navel and the spine can be considered as anchor points of the torso.

10

All participants showed a pattern in which the lines from the indicated location of the tactor on the square board to the actual tactor spot on the observer's body surface seemed to cross at one of two points. One of these points exists for the left and one for the right half of the body, with a mean lateral distance of 6.0 cm between them.
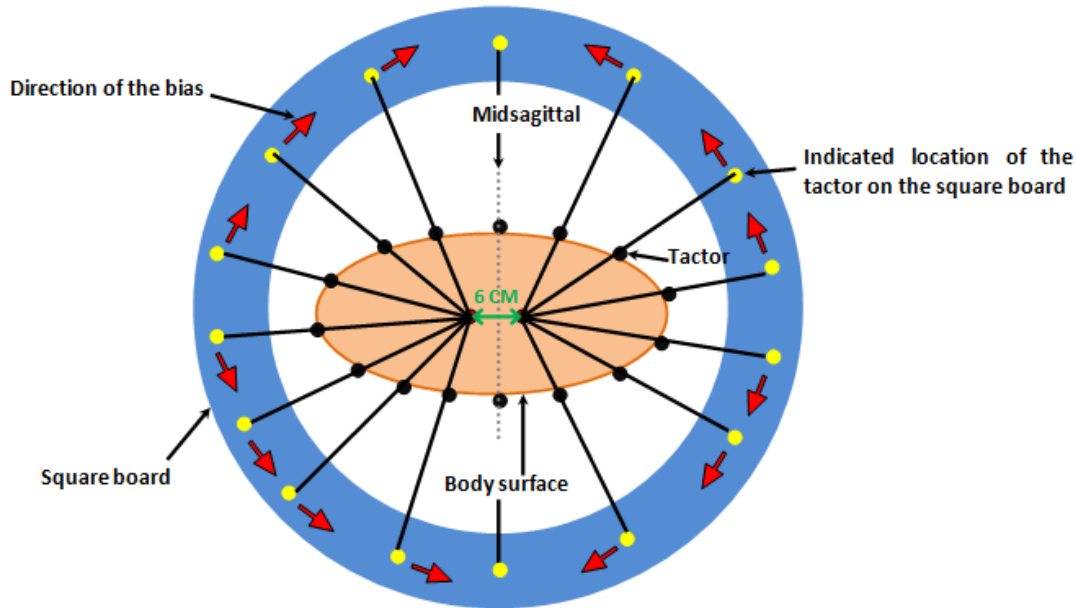
Figure 5: Schematic top view of the Van Erp's experiment and results. Red flashes indicate the direction of the bias in the response of participants. Adapted from Van Erp (p. 307)[22].

Summarizing the findings of the Van Erp [22] experiment resulted in two main conclusions:

1. The navel and spine can be considered anchor points of the torso.

2. There are two internal reference points in the human body, one for each half (left and right), and observers do not use the center of the torso as the origin for observed direction. This suggests that spatial tactile signals should be designed from the internal reference points in the body, and not simply from the midsagittal plane as this reflects how people tend to interpret the signals.

2.4 Vibrotactile Spatial Acuity of the Trunk and Effects of Timing Parameters on Localization Performance

Spatial acuity has been investigated by several methods and most studies have used pressure or brief touches instead of vibrotactile stimuli [18]. Weinstein measured thresholds of two-point discrimination

(minimum distance between two stimuli to be perceived as two distinct stimuli instead of one large stimulus) and tactile point localization on several body locations using pressure stimuli [26]. The lowest thresholds were found for the finger tips and were found to be 2.5 mm for two point discrimination and 1.5 mm for point localization. In contrast, thresholds for the trunk were larger and were found to be around 4 cm for the back and 3.5 cm for the abdomen for two-point discrimination and 10 mm for point localization (for both the back and abdomen). Pressure stimuli are detected by Merkel receptors, but vibrotactile stimuli are detected by Pacinian corpuscles which results in different spatial acuities for the two different types of stimuli. Considering our project uses vibrotactile stimuli on a vest, it would be pertinent to consider the results of the Van Erp [17] investigations about the acuity of the torso in discrimination of vibrotactile stimuli which will be presented in the following sections.

2.4.1 Spatial Acuity by Location

In the first part of the Van Erp's experiments the spatial resolution of vibrotactile stimuli on different locations of the torso was investigated [17]. This was done by placing vertical and horizontal arrays of tactors on the skin of the back and abdomen. In this experiment, each presentation consisted of the sequential activation of two vibrotactors. The experimental task was to indicate whether the second tactor was presented to the left or to the right of the first tactor for the horizontal arrays, and above or below of the first tactor for the vertical arrays.

The results of this experiment demonstrated a uniform acuity of about 2-3 cm across the trunk and there were no acuity differences between horizontally and vertically located arrays. These values are similar to the findings of Weinstein who found spatial acuity of the trunk to be around 3-4 cm for pressure stimuli[26]. The acuity was better for horizontally oriented arrays located on the spine and the navel and was about 1 cm for these regions. This midline accuracy provides further evidence that the spine and the navel can serve as anatomical anchor points as was demonstrated previously by Cholewiak et al.[16], not just because they are anatomical reference points, but because acuity may also be more accurate in these locations. For the design of tactile signals, active tactors should be at least 3 cm apart on the torso, and 1 cm apart on the navel or spine. The navel and spine regions may provide better acuity, reinforcing the idea that these areas may serve as good reference points.

2.4.2 Spatial Acuity and Timing

In the second part of the Van Erp [17] experiment, the effects of the timing parameters on localization performance were assessed. Before we continue, we need to define two concepts:

12

- *Burst Duration (BD):* which is the time between the onset and end of a burst

- *Stimulus Onset Asynchrony (SOA):* which is the time between the onsets of two consecutive bursts

Four pairs of tactors were attached to the back of participants as can be seen in Figure 6. The center-to-center distance between two tactors within a pair was 2.5 cm. The distance between two pairs was 3.5 cm. Each presentation consisted of the sequential activation of two tactors with 25 combinations of *BDs* and *SOAs.* The task of the observers remained the same; participants were asked to indicate whether the second tactor was to the left or to the right of the first tactor. The final results are depicted in Figure 7. Both *BD* and *SOA* were found to affect the localization performance of participants. Performance improved when *BD* and *SOA* increased, and *SOA* was found to have larger effects on performance than *BD*. Therefore, there is a trade-off between the speed of stimulus presentation and spatial acuity. Hence, applications which utilize tactile displays and require high spatial acuity can profit from longer *BDs* and *SOAs,* and tasks that depend on fast response times should make use of larger distances between the vibrotactors [17].
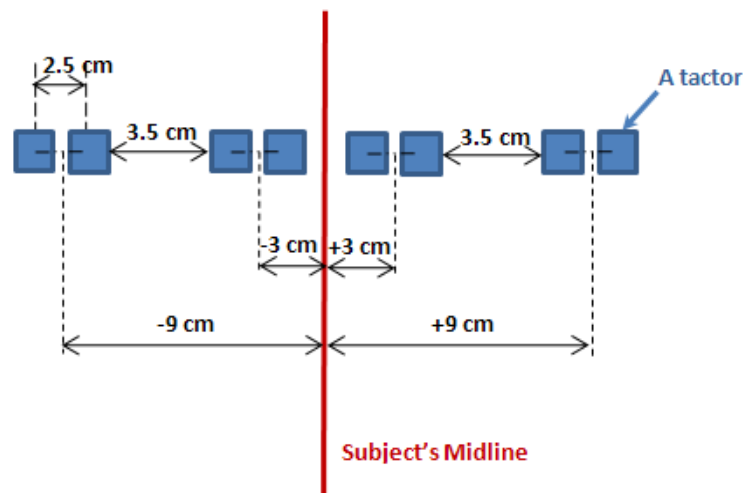
Figure 6: Placement of Tactors for Van Erp Experiment [17]**.**

Summarizing the results of the Van Erp experiment [17], we can derive two main conclusions:

1. Spatial acuity is relatively uniform over the trunk and it is approximately 2-3 cm for vibrotactile stimuli. This acuity is better for horizontally oriented arrays located on the spine and navel and is about 1 cm for these regions.

2. Localization performance improves when *BD* and *SOA* of two sequentially activated vibrations increase.
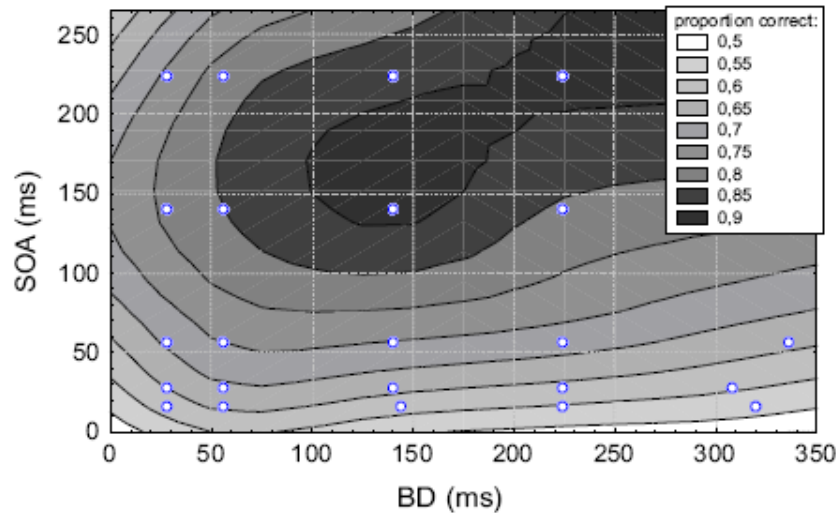
Figure 7: Effects of the timing parameters on localization performance. Proportion correct as function of BD and SOA. Darker colors indicate better performance. Figure taken from Van Erp (p. 83)[17].

2.5 Guidelines for Coding Information through Vibrotactile Displays

The sense of touch is a unique communication channel and vibrotactile displays transfer information by presenting vibrations through this channel. The interest in application of vibrotactile displays is growing, and these displays have already been used in a number of applications. They have been used as a sensory substitution for people with visual or hearing disabilities. For example, Optacon is a device that translates written text into vibrotactile signals through an array of pins in contact with the user's finger [27], [28], [29]. Tactile displays have also been used to assist operators with orientation and navigational tasks in situations where disorientation occurred due to mismatched vestibulo-ocular response and the absence of stable frames of reference [2], [6], [7], [8]. There are also many tactile interfaces which are being used for exploring computer-generated virtual environments [30].

Considering the many possible applications of vibrotactile displays, an investigation of different methods of information representation and coding principles (how to develop tactile patterns that can be

14

understood within a specific application) would be pertinent. The focus of the following subsections is on how different tactile parameters can be manipulated to present messages in vibrotactile displays.

2.5.1 Coding Information by sing Different Frequrncies

Optimal sensitivity of human skin to vibration is within 150 to 300 Hz [31]. For frequencies outside of this interval, the displacement of the skin must be greater to be detected. The amplitude required for detecting vibration at any given frequency varies for different locations on the body. Wilska [32] measured detection thresholds of 25-1280 Hz vibrations for different locations on the body. He found the lowest threshold amplitudes within the frequency range 200-450 Hz. For 200 Hz vibrations, the finger tips have the lowest threshold of 0.07 μm, whereas in the abdominal and gluteal regions the lowest detection threshold is as high as 14 μm [15].

Verrillo [33], [34] measured the sensitivity to vibration on the glabrous skin of the hand as a function of frequency, tactor properties, and differences in the pressure upon the skin. Based on the results, the detection threshold as a function of frequency was found to be a U-shaped curve which has its minimum in the region of 250Hz. He also demonstrated that threshold decreases as the vibrating contactor, the portion of the tactor in contact with the skin, pressed further into the skin. In another experiment, Verillo concluded that the size of the area of stimulation is a significant parameter of a vibrotactile stimulus. When the area was reduced, higher thresholds of detection were recorded [35]. Cholewiak et al. [16] measured vibrotactile detection thresholds as a function of stimulus frequency by presenting stimuli on 6 equidistant locations on a vibrotactile belt which encircled the abdomen. They reported that there is no statistically significant difference between vibrotactile detection thresholds around the trunk. A vibrotactile stimulus at a given frequency was perceived similarly at spine, navel and four additional loci on the sides of the abdomen. Figure 8 shows the results of this experiment. Taken together, these results suggest that tactors do not require additional compensation or tuning to achieve similar levels of perceived vibration when used in the tactor vest.

There are no extensive studies on the ability for individuals to discriminate between different frequency levels of vibrotactile and we have relatively little data on this topic. Therefore it is difficult to specify distinct changes in vibrotactile frequency that could be correctly distinguished by operators[31]. Rothenberg, Verrillo, Zahorian, Brachman, and Bolanowski [36] suggested that an appropriate scale of vibration frequency may include approximately seven differentiable levels from the lowest to the highest applicable values on the forearm. Sherrick [37] presented vibrations to the finger and reported that within

the frequency range of 2-300 Hz, between three to five levels of vibrotactile frequency can be discriminated by humans, and this can be increased up to eight recognizable levels when intensity is added as a redundant cue. He also found that discrimination above 100 Hz deteriorates rapidly. The results of this study also state that a low frequency vibration at high intensity can be incorrectly perceived as a moderate vibration at medium intensity. This highlights the fact that increasing the amplitude of a vibration also increases the perceived frequency of the signal [31].
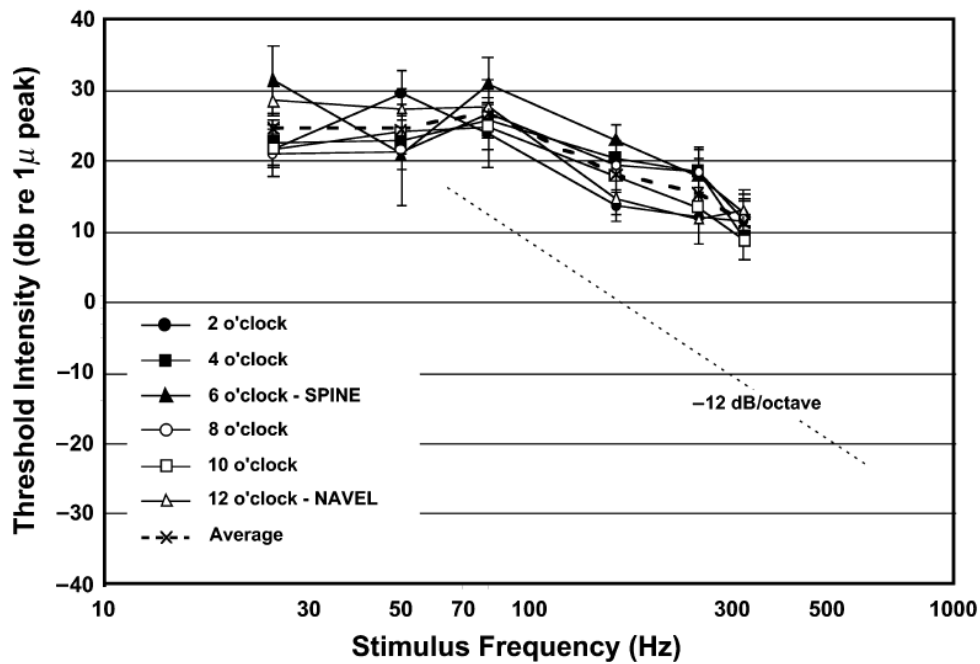
Figure 8: Vibrotactile detection thresholds measured at six locations around the abdomen. Figure taken from [16] (p. 973).

Other studies have suggested that a maximum of nine different levels of frequency should be used for coding information [38], [25]. Also, differences between frequency levels for vibrations with equal amplitude should be at least 20% [38]. Brewster and Brown [25] also state that "the number of frequency steps that can be discriminated also depends on whether the vibrotactile cues are presented in a relative or absolute way. Making relative comparisons between stimuli is much easier than absolute identification, and this will lead to much fewer discriminable values." It should be noted that for areas with less sensitivity and lower density of innervations like the trunk, increases in the perceived frequency grow more rapidly with increases in frequency of the physical stimuli [31].

16

The Weber Fraction is a formula that is often used to determine the minimum threshold of perceived change in any parameter (e.g., amplitude, frequency, weight). For frequency, it is the differential threshold divided by the reference frequency, expressed as a percentage.

$$k = \frac{\Delta I}{I}$$

(1)

Where *K* is the Weber Fraction, *I* is the reference amount of the parameter and *ΔI* is the minimum threshold of the perceived change in a parameter (e.g. frequency). The Weber fraction is reported to change as a function of frequency. However, different results are reported from different authors. In one study the Weber fraction increased from about 18% at low frequencies to 30% at 300 Hz, whereas in another study it decreased from 30% at low frequencies to 13% at 200 Hz [31].

Summers et al. [39] investigated the perception of step changes in stimulus frequency. The stimuli were periodic signals of 80, 160, 240, and 320 ms durations with one octave step change of frequency at their halfway point. For example a signal of 240 ms duration was increased/decreased one octave in its frequency after 120 ms from its onset. There were also constant stimuli with no step change. Three different waveform types were used for this experiment: sine wave, monophasic pulse, and a tetra phasic pulse. Figure 9 illustrates these waveforms. Vibrations were presented at two different sensation levels, 24 dBSL and 36 dBSL. The experiment showed that participants were able to correctly detect constant stimuli, but with increasing or decreasing frequency of the stimuli there were more unsuccessful discriminations as shown in Figure 10. The results of the experiments also revealed that the effect of waveform type was not very significant.

Sine Wave   Monophasic Pulse   Tetraphasic Pulse
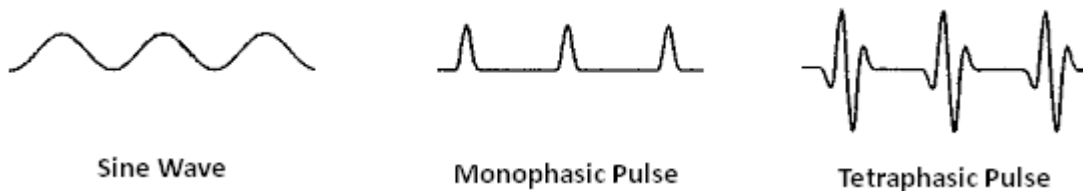
Figure 9: Three types of waveforms used in the Summers et al. experiment [39]. Adapted from Summers et al[39]. (p. 3687)

Due to the large amount of variation and uncertainty about the perception of changes in frequency, changes in frequency may not be a useful method for presenting messages in vibrotactile displays. Also, the limited bandwidth of frequency of electrical devices and tactors may limit the display when

information is coded using different frequency levels. Therefore frequency should be cautiously changed in these displays, especially when amplitude is also being manipulated as a variable [31].
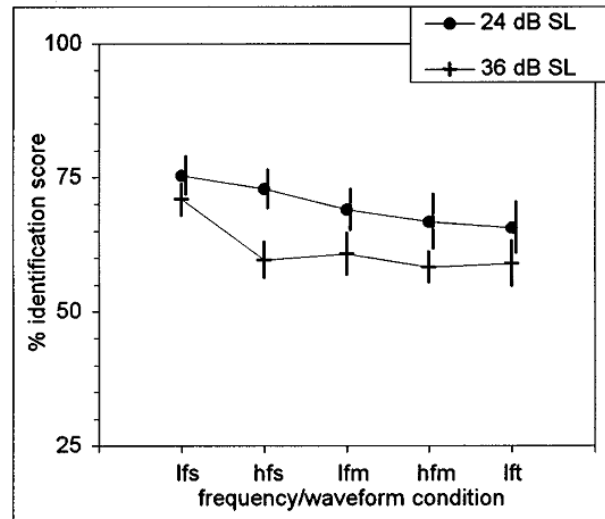
Figure 10: Overall results of the Summer et al. [39]experiment. lfs = 50/100Hz sine; hfs = 200/400Hz sine; lfm = 50/100Hz monophasic; hfm = 20/400Hz monophasic; lft = 50/100Hz tetraphasic. Figure is taken from Summers et al.[39] (p. 3690).

2.5.2 Coding Information by using Different Amplitudes

Changes in amplitude of vibration can be a very useful parameter to encode information in vibrotactile displays [4]. For example, the urgency of a message can be represented by presenting vibrations with different amplitudes to the operator's skin. Therefore, it is important to know how individuals are able to perceive different amplitudes of vibrations in terms of intensity or magnitude. One of the units of measurement for amplitude is decibels above sensation level (dBSL). It measures the amplitude of a signal relative to an individual's sensation threshold. For example, if a person's minimum sensation threshold is 20 dB and a signal is at 40 dB, the sensation level of this signal for this individual is 20 dBSL. Craig [40] measured the difference threshold (the minimum change in amplitude that can be discriminated by an individual 50% of the time) of a 160 Hz vibration presented to the right index finger. The signal was raised to 14, 21, 28, and 35 dBSL. He found that the difference threshold at these levels is constant and is approximately 1.5 dB. Craig [40] also found that the difference threshold increases with decreasing intensity below 15 dBSL.

18

Verrillo et al. [41] measured contours of equal-sensation of magnitude judgments, resulting from the interaction of frequency and amplitude. The stimuli consisted of 10 different vibrotactile frequencies and were presented by a 2.9 cm2 contactor to the thenar eminence (i.e. palm) of the right hand. The experiment consisted of two main sections. In the first section, a series of 10 stimuli (one for each of 10 different vibration frequencies) with different amplitudes were randomly presented. Participants were instructed to assign numbers to each presented stimulus (magnitude estimation). In the second section, participants could control the amplitude of vibrations by means of a control knob. They were instructed to adjust the amplitude of the vibration such that its magnitude subjectively fit the numbers that had been presented to them (magnitude production). These are both techniques that are often used in psychophysics.

(a)   (b)

Figure 11 illustrates the results of the magnitude estimation and magnitude production procedures for a 25 Hz vibration.
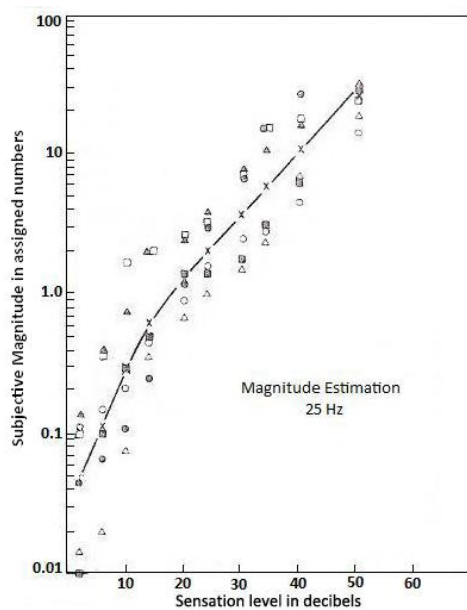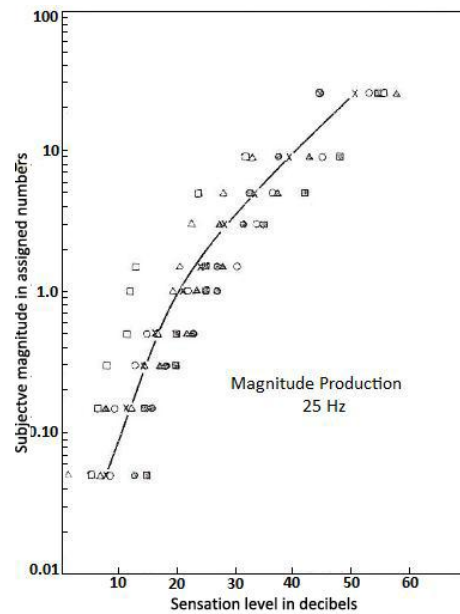
(a)   (b)

Figure 11: Results of magnitude estimation (a) and magnitude production (b) for a 25Hz vibration for different participants. Solid lines illustrate geometric means. Figures adapted from Verrillo et al [41] (p. 368).

19

For each frequency tested, the geometric mean of the individual responses for the magnitude estimation and magnitude production functions were calculated. These functions were averaged, and curves of numerical magnitude balance were obtained. The curves in Figure 12(a) indicate that the perceived intensity of a vibratory stimulus at a given frequency grows as a power function of the stimulus amplitude. The exponents found for the power function were 0.89 for 25-300 Hz, 0.95 for 500 Hz, and 1.2 for 700 Hz vibrations. Stevens' findings [42] also provide further evidence that the perceived intensity of a vibratory stimulus grows as a power function of stimulus amplitude. The slope of this function increases more rapidly on locations with lower sensitivity to vibration, such as torso. Taken together, this suggests that changes in the amplitude of a vibrotactile are perceived to be greater on the torso [31]. All of the experiment results from both sections of the Verillo et al. [41] were collected and re-plotted in terms of displacement as a function of frequency. The resulting set of curves is presented in Figure 12(b), and illustrates the contours of equal-sensation of magnitude. According to these curves, the intensity of a 250 Hz vibrotactile with specific amplitude can be identically perceived as a vibration at lower/higher frequency with higher amplitude. The results from the mentioned studies reveal the fact that there is a large interaction between frequency and amplitude of a vibrotactile stimulus. Therefore it is recommended that only one of these parameters should change when using vibrotactile displays [31].

(a)   (b)
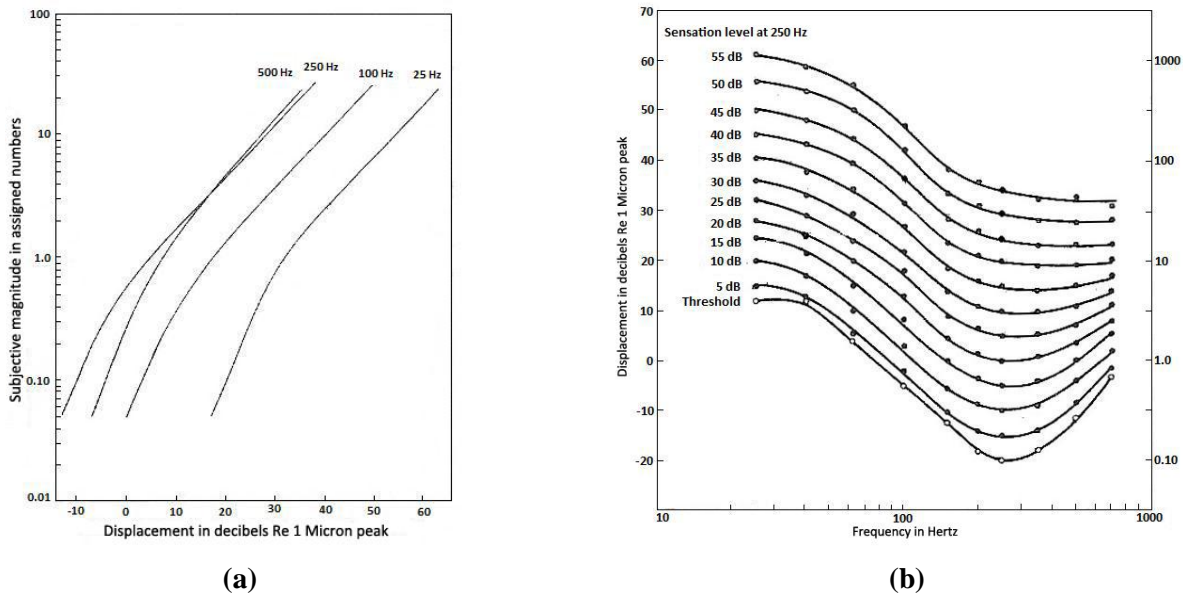
Figure 12: Subjective magnitudes as a function of absolute displacement (a), Contours of equal sensation magnitudes, the sensation level indications refer to a signal at 250Hz (b). Figures adapted from Verillo et al. [41] (p. 370-371).

2.5.3 Coding Information by using Different Durations of Vibrotactile stimuli

Different durations of vibratory stimuli can also be used to encode information in vibrotactile displays. Summers et al. [39] found that performance for detecting increasing or decreasing frequency in a vibrotactile stimulus improves as stimulus duration is increased from 80 to 320 ms. When vibrotactile stimuli are used to present a simple alert, the preferred duration of tactile stimuli is between 50 and 200 ms. Prolonged vibrations are reported to be annoying for users [43]. However, vibrations with different durations can be aggregated to provide rhythmic units [25], [44]. Brown et al. [44] provided three different rhythms by grouping pulses of different durations together. They used these rhythms to present three different types of messages. They reported that participants were able to correctly recognize the three message types with an average accuracy of 93%. Van Erp [38] also suggests that **when a single vibrator is used to encode information in a vibrotactile display, the time between signals must be at least 10 ms.**

2.5.4 Coding Information using Different Locations for Vibrotactile Stimuli

A vibratory stimulus exerted to the trunk can be localized with relatively high accuracy and reliability [16], [22]. Therefore, arrays of vibrotactors can be used to support a number of spatial orientation applications, such as representing the location of an object relative to the body, presenting directions in navigation systems, or as a counter measure for spatial disorientation [22], [45]. In general, observers are more capable of correctly localizing stimulus near the spine and navel on the torso. These points can serve as anatomical reference points (anchor points) for the trunk [16]. There is a bias between the actual tactor location and the responses of observers regarding the location of the stimuli. This bias is toward the midsagittal plane (toward the navel for the front of the torso and toward the spine for the back of the torso) [22].

The ability of participants to localize a vibrotactile stimulus in a 3×3 tactor array was investigated in an experiment by Linderman and Yanagida [46]. The vibrotactor array was affixed to the backrest of an office chair, such that vibrations were presented to the lower back region of the participant's torso. The spacing between the centers of each pair of neighbouring tactors was 6 cm. Lindeman and Yanagida found that participants were able to report the correct location of the tactors with an accuracy of 84% [46]. In addition, they found that the spacing between tactors influenced the localization accuracy and must be adjusted carefully in the design of vibrotactile displays. This is especially true when they are being used to convey spatial information. It is recommended that the inter-tactor spacing on the skin be

greater than the two-point threshold for vibration [31]. As stated in Section 3.3, **the inter-tactor spacing on the trunk should be at least 3 cm for better localization performance** [17].

2.6 Vibrotactile Patterns

The current literature suggests that vibrotactile patterns can be classified based on the number of tactors used into two main groups: spatio-temporal patterns and tactons. Spatio-temporal patterns can be generated by sequentially activating a series of vibrotactors and require more than a single vibrotactor. Tactons, on the other hand, consist of a single vibrotactor and are manipulated by turning the tactor on and off. These two types of patterns are discussed in detail in the following subsections.

2.6.1 Apparent Movement and Spatio-Temporal Patterns

Spatio-temporal patterns and perceptions of apparent movement can be generated by sequentially activating a series of vibrotactors placed on the skin. Resulting patterns can be used to intuitively present information regarding orientation or direction of external events. Cholewiak and Collins [47] investigated the influences of timing parameters and presentation modes on the generation of vibrotactile patterns. In this study, patterns were presented to the distal pad of the left index finger, the left forearm and the lower back region by means of seven vibrotactors for each area. Two modes of pattern presentation were used; saltatory and veridical. In veridical mode, all seven of the vibrotactors that were situated in a linear array were activated in sequence to provide a linear pattern. In salutatory mode, seven bursts of vibration were presented at only three tactor sites. Three bursts of vibration presented through the first; three bursts through the fourth; and one burst through the seventh vibrotactor. Figure 13 illustrates the concepts of these presentation modes. The distance between the adjacent tactors was 2.54 mm on the finger tip and 15.24 mm on the forearm and the lower back. The vibrotactors which were used for the fingertip were smaller in size than those were used for the forearm and the lower back. The vibrations were presented in the two modes with different BDs and IBIs (Inter Burst Interval). The values for the BDs and the IBIs were 4, 9, 17, 26, 35, 70, and 139 ms. The experiment was done in two main parts. The main goal of the first part of the experiment was to find out how efficiently a line could be generated. Participants were instructed to rate the levels of perceived length, smoothness, spatial distribution, and straightness of the presented patterns.

During the second part of the experiment, vibrations were presented only to the lower back. The aim of the second experiment was to find out to what extent are participants able to differential between the two

presentation modes (veridical and salutatory), and which of these modes can generate a better sensation of a line.

The results of the first experiment showed that when vibrations were presented with longer BDs, participants perceived longer lines. Significant interaction between BD and IBI was also found. With longer IBIs for stimuli with a given BD, the generated lines were reported to have longer length. This means that as the velocity of activation sequence increases, the perceived length of the pattern decreases. The stimuli were also perceived to be smoother with shorter IBIs. Perceived smoothness of patterns was found to be mainly a function of IBI. Perceived spatial distribution was reported to have better quality when small BDs and IBIs were used. Finally, judgments of straightness improved with shorter BDs and shorter IBIs which indicates that increased velocity of an activation sequence will result in judgments of straighter patterns. This finding is in consent with the findings of Langford, Hall, and Monty [48]. A line produced by a moving point across the skin appears to wander at lower speeds and it is perceived to be straight at higher speeds [48]. The results of the second portion of the experiment revealed that the verdical mode was superior to the salutatory mode, but the differences were very small.
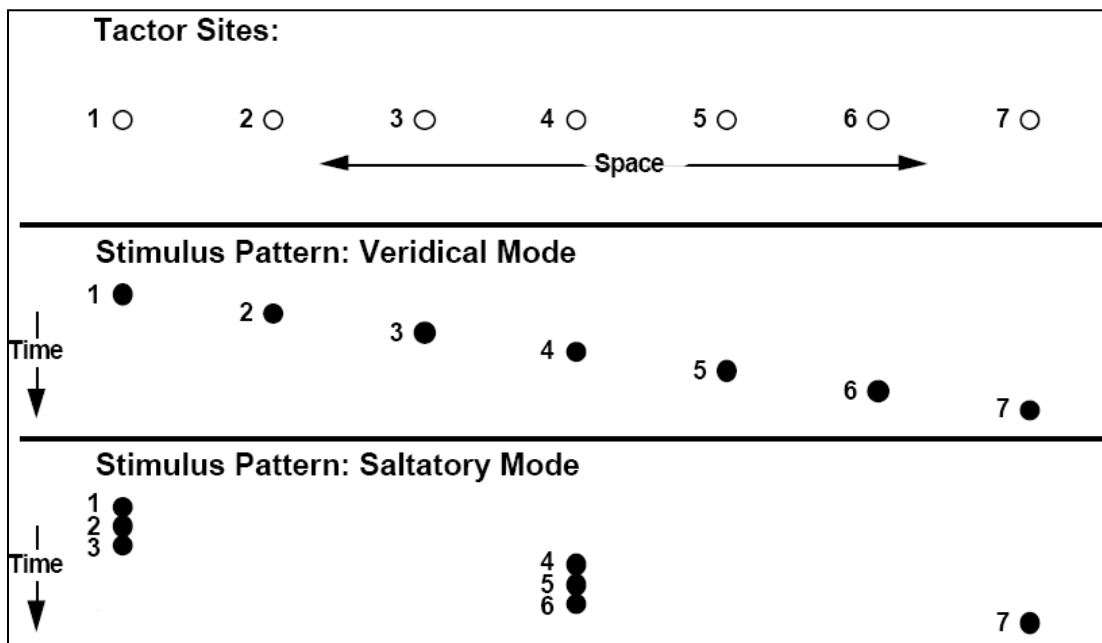
Figure 13: Concepts of veridical and saltatory presentation modes. Figure adapted from Cholewiak and Collins [47] (p.1223).

In addition to the apparent movement illusions explained above, the simultaneous activation of two vibrotactors located spatially close together causes the sensation of only a single point between the two tactors (apparent location). This point shifts continuously toward the vibration with higher intensity [49]. Kirman [50] investigated the effects of stimulus onset asynchrony (SOA) and stimulus burst duration (BD) on vibrotactile apparent movement. Vibrotactile stimuli were presented to two different locations on the right index finger. The vibrations were varied in both duration and the inter-stimulus onset interval. They were presented in 6 durations (1, 10, 20, 50, 100, and 200 ms) and were combined with each of 10 SOAs (10, 20, 30, 50, 70, 90, 110, 130, 150, and 200 ms). Therefore a total of 60 pairs of stimuli were presented to the participants. Kirman [50] found that the quality of perceived apparent movement varies as a function of SOA. Figure 14 shows this function for stimuli with durations of 200 ms. The best feeling of apparent movement for the two stimuli was achieved when the inter-stimulus onset interval was approximately equal to 130 ms. This means that the second stimulus started to stimulate 130 ms after the onset of the first stimulus. This also resulted in a 70 ms overlap between the two stimuli.
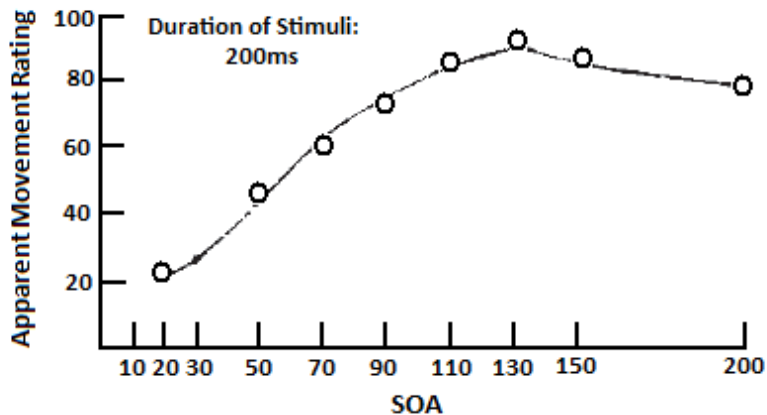
Figure 14: Apparent movement rating as a function of SOA. Figure adapted from Kirman[50] (p. 2).

Figure 15 shows the optimal SOAs for different stimuli durations applied in the experiment. As can be seen in the figure, participants were able to optimally perceive apparent movement when the SOA were 70, 50, 50, 70, 90, and 130 ms respectively for stimuli with durations of 1, 10, 20, 50, 100, and 200 ms respectively.

Finally, Figure 16 shows the judgments of apparent movement for the optimal SOAs as a function of stimulus durations. According to this figure, as stimuli duration increases, judgments of apparent

24

movement increase for optimal SOAs. Taken together, the results of this study suggest that when spatio-temporal patterns are used in vibrotactile displays, the quality of perceived apparent movement is a function of inter-stimulus onset interval and burst duration.

While designing vibrotactile displays, it is important to remember that the number of patterns that can be generated is dependent on the number of arrays of vibrotactors embedded in the display. Jones, Lockyer, and Piateski [51] presented navigational direction messages to participants through a set of vibrotactile patterns. The patterns were presented using a 4×4 tactor array mounted on the lower back of the participants.
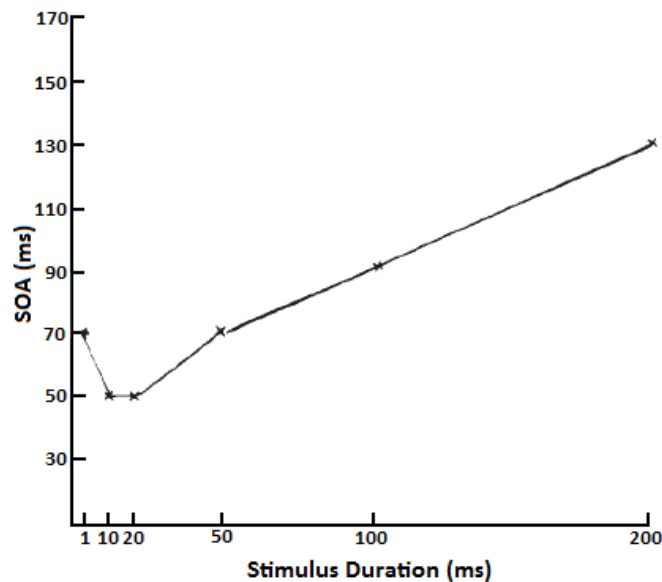
Figure 15: Optimal SOA as a function of stimulus duration. Figure adapted from Kirman [50](p. 3).

The participants navigated through a path designated by a grid of cones. Jones et al. [51] found that participants were able to accurately follow the navigational commands to walk through the course using this aid. A visual depiction of one of the vibrotactile navigational commands is illustrated in Figure 17. Yanagida, Kakita, Lindeman, Kume, and Tetsutani [52] investigated the participant's ability to recognize patterns which were used to present English letters and numbers. The patterns were presented through a 3×3 tactor array affixed to the backrest of an office chair. The sequential presentations of the patterns were such that they traced the trajectory in a manner that simulated hand writing on the back. Yanagida et al. [52] found a ratio of 87% correct letter or number recognition. Although letter recognition was relatively successful in this experiment, it should be noted that in high workload conditions the accuracy

may not stay the same. In the Yanagida et al. [52] experiment, participants were not asked to perform any additional tasks beyond the recognition task. Thus, the workload for the participants was relatively low.
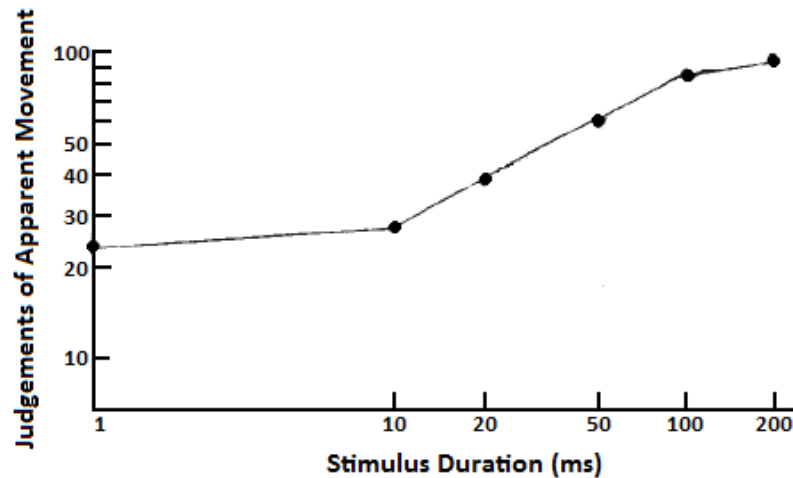
Figure 16: Judgments of apparent movement for the optimal SOAs as a function of stimulus duration (results of Kirman experiment). Figure adapted from Kirman [50](p. 5).
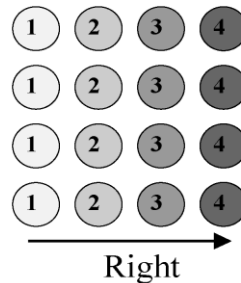
Right

Figure 17: The pattern generated through a 4×4 array of vibrotactors for "turn right" command. The arrow represents spatial order of activation of tactors. Figure adapted from Jones et al.[51] (p. 1367).

It should be noted that the participant's familiarity with the displayed set of patterns may also affect the accuracy of the pattern recognition process. Therefore, practicing may improve the discrimination performance for vibrotactile patterns [20], [52].

2.6.2 Tactons

Vibrotactile patterns can also be generated by means of a single tactor. These patterns are called Tactons. Tactons are brief messages that can be used to represent complex concepts and information in vibrotactile displays. They are tactile replication of icons or earcons [25], [44]. Brown et al. [44] generated tactons by

26

using different rhythms and waveforms. As mentioned previously, vibrations with different durations can be grouped together to create rhythmic units. Complex waveforms can be generated using sinusoidal amplitude modulation, as illustrated in Figure 18.

The feeling of roughness can be transmitted by presenting participants with amplitude modulated signals through vibrotactors [44]. Brown et al. [44] found that participants are able to differentiate different amplitude modulated signals in terms of roughness. Sine waves with no modulation are perceived as being smoother, and the feeling of roughness increases as modulation frequency decreases. Brown et al. [44] preferred not to use vibrotactile parameters such as frequency or amplitude for creating tactons. The limited bandwidth of tactors and electrical devices discourage the use of different levels of frequency. Reducing the amplitude may make the pattern undetectable and increasing amplitude may cause pain and cause annoyance [44].

(a)   (b)
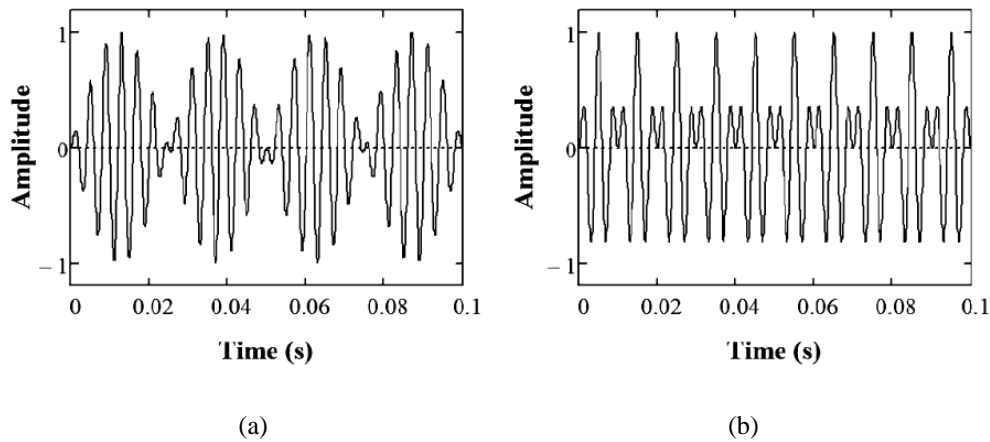
Figure 18: 250Hz sine wave modulated by 20 Hz (a) and 50 Hz (b) sine waves. Figures adapted from Jones and Sarter [31](p. 104).

Brewster and Brown [25] categorized tactons in three main groups; compound tactons, hierarchical tactons and transformational tactons. Brown et al. [44] investigated the ability of a group of participants to identify different rhythms and different roughness levels when the characteristics are combined together to form transformational tactons. A single C2 tactor was used in the experiment. Three types of alerts (voice call, text message and multimedia message) were encoded using different rhythms. The priority of the alerts (low, medium or high) was encoded using different roughness levels. For example, the same rhythm was used to present a high priority text message and low priority text message, but they were

27

presented with different roughness levels. Brown et al. [44] found average discrimination rates of 93% and 80% for the different alert types (represented by different rhythms) and alert priority levels (represented by different roughness levels) respectively. The average result for overall tacton recognition was 71%. Considering these results, we can conclude that in vibrotactile displays, tactons can effectively convey complex messages to the operators in a very concise manner.

2.7 Other Reviews of Tactile Characteristics

Many other researchers have reviewed coding principles and characteristics of vibrotactile stimuli. One recent review by Self, van Erp, Eriksson, and Elliott [53] discussed nine tactile characteristics which designers may be able to manipulate in order to communicate messages. While many of these have been discussed above, a table (taken from Self et al. [53] is included below to show some other possible methods of coding information into the tactile modality.

Table 1: Tactile Characteristics [53] (p. 4)

Characteristic	Properties
Size	- Limited number of distinctive levels - Large difference between sizes preferable - A clear boundary is needed - Simultaneously displayed sizes is feasible
Shape	- Fair number of distinctive levels - Similar tactile shapes should be avoided - A clear boundary is needed - Simultaneously displayed shapes is feasible
Orientation	- Many distinctive levels possible - Large distance between displays preferable - Simultaneously displayed positions is highly feasible
Position	- Many distinctive levels possible - Large distance between displays preferable - Simultaneously displayed positions is highly feasible
Moving patterns	Any distinctive levels possible

28

	• The moving patterns should be quickly recognizable after their start
	• Simultaneously displayed moving patterns is moderately feasible
Frequency	• Limited number of distinctive levels
	• Low feasibility for simultaneously displayed frequencies
Amplitude	• Limited number of distinctive levels
	• Low feasibility for simultaneously displayed amplitudes
Rhythm	• Many distinctive levels possible
	• The rhythms should be quickly recognizable after their start
	• Low feasibility for simultaneously displayed rhythms
Waveform	• Includes square, triangular, saw tooth, and sine waves
	• Requires sophisticated hardware

2.8 Masking Effects

Masking occurs when two stimuli are presented close to each other in space or time and decrease the detectability of each other. It is the difference between the perception of a stimulus when it is presented solely, and the perception of the same stimulus when it is presented close to another stimulus, either in time or space. In the design of vibrotactile displays, masking effects can play a large role in how operators perceive the messages. It is possible that an operator might miss an important piece of information due to masking by a nearby tactor, especially if multiple streams of data are presented through the vibrotactile display.

In general, we use the term "target" for the stimulus which is to be identified, and the term "masker" for the stimulus which is to be ignored. The masker stimulus may change several discriminating parameters of the target stimulus (e.g. sensation threshold, difference threshold and perceived location of the stimulus) [14].

2.8.1 Temporal Masking

Temporal masking occurs when the vibrations are presented to the same location, and the target stimulus is presented either within the time interval of the masking stimulus, or near the onset or just after the offset of the masking stimulus. Temporal masking decreases when the temporal separation between the onsets of stimuli increases [38], [14]. Forward masking occurs when the target stimulus is corrupted with a preceding masking stimulus. Backward masking occurs when the target stimulus is corrupted with a

subsequently presented masking stimulus. Participants are better able to recognize tactile patterns when they are presented in isolation than when they are presented with a forward or backward masker. Higher masking levels occur at shorter SOAs [54]. Craig and Evans [54] presented a masker pattern followed by a target pattern to participants who were instructed to identify the second pattern while ignoring the first pattern. They found that with shorter SOAs there was more backward masking than forward masking. As SOAs increased, forward masking decreased more gradually than backward masking. Craig and Evans [54] also reported that with long SOAs, the opposite was true and there was more forward than backward masking. Forward masking remained visible for SOAs up to 1200 ms.

In another study, Gescheider, Bolanowski, and Verrillo [55] investigated the amount of simultaneous, forward, and backward masking. In this experiment a 700 ms vibratory stimulus was used as the masker, and a 50ms vibration was used as the target. The SOA was varied over a range of 2000 ms. The target stimulus was presented within the time interval of the masking stimulus (simultaneous masking), presented with partial overlap with the masking stimulus, or without any overlap with masking stimulus (forward and backward masking). The effect of temporal masking was strongest when the target stimulus was presented near the onset or just after the offset of the masking stimulus. The amount of masking declined as the time interval between masking and target stimuli increased. The rate of decline of the masking effect appeared to be same for forward and backward masking. Despite the findings of Craig and Evans [54], they did not report the persistence of forward masking for long SOAs. This difference between the results is probably due to the different methodologies used. As mentioned previously, Craig and Evans [54] used patterns of vibration in the form of vertical or horizontal lines as stimuli, whereas Gescheider et al. [55] used single vibrations as stimuli. Unfortunately, we cannot make any strong conclusions regarding temporal masking based on the current literature.

2.8.2 Spatial Masking

Spatial masking occurs when two stimuli are presented to two distinct locations at different or overlapping times [38], [14]. We can reduce the amount of spatial masking by increasing the distance between stimulated sites [14], [56]. When stimuli are presented at different times, spatial masking occurs only when the target and the masker stimuli are both high frequency vibrations. Therefore the effect of spatial masking is greater on receptors within the Pacinian system. Non-Pacinian systems do not demonstrate this characteristic, unless the stimuli are presented at the same time [57]. Craig [58] measured the difference threshold in the presence and absence of a masking stimulus. When the

difference threshold was measured in the presence of the masking stimulus, a masking vibration was presented simultaneously with the test stimulus. The test stimulus was a 160 Hz vibration presented to the right index finger. The masking stimulus was a vibration with the same frequency delivered to the right little finger. The results of this experiment demonstrated that the difference threshold of the target stimulus considerably increases as the intensity of the masker stimulus increases. Only when the intensity level of the target stimulus was more than 15 dB above threshold, the difference threshold in the presence of the masking stimulus was similar to the difference threshold in the absence of masking stimulus. In order to reduce the negative effects of spatial masking, it is recommended that vibrotactors which have a static surround in their structure should be used (e.g. C2 tactors). A rigid surround can prevent the spread of vibrations and surface waves to adjacent locations reducing the effect of spatial masking [38], [56].

2.9 Tactile Perception Summary

Before we move onto the display`s hardware design and fabrication and evaluation of the applied vibrotactors, we summarize the findings discussed. The art of designing vibrotactile displays is still in its infancy. Currently, one important focus in the design of such displays is their capability in navigation tasks in 3D space. The three-dimensional nature of the torso can facilitate the understanding of three-dimensional spatial information. Most researchers who have investigated the localization ability and spatial acuity of the skin for vibratory stimuli have used a single array of vibrotactors. There are relatively few studies which have examined these abilities while using multiple rows of tactors. Other uses of tactile displays such as alerts and other methods for coding other types of non-spatial information are also actively being explored. Human factors issues have major influences on design and application of any vibrotactile display. Therefore, we should consider the perceptual factors in pattern generation and coding procedures used to design future vibrotactile displays. Relevant guidelines for different ways of information presentation on these displays are provided in this section.

We can code information by presenting vibrations with different frequencies, amplitudes, durations, and locations on the body. The optimal sensitivity of human skin to vibration is between 150 to 300 Hz. The detection threshold as a function of frequency is a U-shaped curve which has its minimum in the region of 250 Hz. High levels of interaction between frequency and amplitude of a vibrotactile stimulus suggests that only one of these parameters should be changed for coding information. Also, there is a high level of uncertainty about the perception of change in frequency by human skin. Changes in the amplitude of vibration can be perceived with relatively good accuracy which makes it a very useful parameter to

31

encode information in vibrotactile displays. Vibrations with different amplitudes can be used to create different levels of intensity. Different durations of vibratory stimuli can also be used to encode information. When a vibrotactile stimulus is being used to present a message, the duration of vibration should be between 50 to 200 ms. Prolonged vibrations are annoying for users. Also, vibrations with different durations can be grouped together to provide rhythmic units which can be used to generate tactons.

A vibratory stimulus exerted to the trunk can be localized with relatively high accuracy and reliability. This fact makes the location of a vibration an important parameter for coding information in vibrotactile displays. In general, observers are more capable of correctly localizing stimulus near the spine and the navel on the torso. These points can serve as anatomical reference points (anchor points) for the trunk. We should consider taking advantage of these anatomical points of reference for coding information in a vibrotactile torso display. For better localization performance, the inter-tactor spacing on the skin should be greater than the two-point threshold for vibration. For the trunk, the inter-tactor spacing should be about 3 cm.

Based on the number of tactors employed to represent messages in a tactile display, vibrotactile patterns can be divided into two main groups: *tactons* and spatio-temporal patterns. *Tactons* can effectively convey abstract messages to the operators by means of a single tactor. Spatio-temporal patterns can be generated by sequentially activating a series of vibrotactors and can be used to intuitively present information regarding orientation, direction, or more abstract concepts. Obviously, the number of distinctive patterns that can be generated through a vibrotactile display is dependent on the number of arrays of tactors in the display. Therefore, spatio-temporal patterns provide a larger set of possible discriminable patterns than tactons.

It should also be noted that when information is being presented through a vibrotactile display, all of the tactors must have proper contact with the skin, such that the vibrating contactor (the part of the tactor that makes contact with the skin) maintains contact with the skin. Otherwise, part of the message may be missed or a tactile pattern may be incorrectly perceived as a different but similar pattern.

In order to produce different driving electrical signals for the vibrotactors which are used in the vibrotactor vest, we require a controller hardware. In the next chapter we provide descriptions about the design of such a controller.

32

Chapter 3

Hardware Design and Fabrication

3.1 Introduction

Tactile displays are usually comprised of vibratory stimulators which are arranged in specific formation based on the application of the display. One of the vibrotactile stimulators that have been used in several studies is EAI's C2 Tactor [59], [16], [25]. The C2 tactor is a miniature vibrator which is also used in our tactile vest.

As mentioned previously, different tactile parameters can be manipulated to present different messages in vibrotactile displays. According to the datasheet of the C2 Tactor (see appendix A) [59], the electrical resistance of a C2 Tactor is 7 ohms and its minimum recommended driving signal is a 250 HZ sine wave at 350 mA. The maximum suggested electrical current to activate this tactor is 500mA [60]. Although the recommended driving signal for a C2 Tactor is a 250Hz sine wave at 350 mA, it can also be driven through electrical signals which are different in terms of waveforms, amplitudes and frequencies. In order to produce the different driving electrical signals we require a controller hardware which has the following specifications:

1- Can be easily controlled through a PC.

2- Be capable of providing different electrical signals with different waveforms (Sine wave, Triangle wave, Saw-tooth wave and Square wave), frequencies (50 - 700 Hz range) and amplitudes (3, 3.5, 4 and 4.5 Volts).

Therefore, the controller hardware should be comprised of three main parts:

1- A controllable digital unit with the capability of producing signals which are different in terms of waveform (Sine wave, Triangle wave, Saw-tooth wave and Square wave), and frequency (50 - 700 Hz range). This piece of hardware should be such that it can be connected to a pc to receive commands and produce desired outputs;

2- A digital to analogue converter to convert the generated digital signals to analog waveforms;

3- A power amplifier to provide the requiring power to drive the C2 tactors;

The outline of the desired controlling hardware is sketched in the Figure 19. A microcontroller board equipped with an analogue to digital converter and a power amplifier on its output was used to provide the required driving electrical signals.

Controllable digital unit
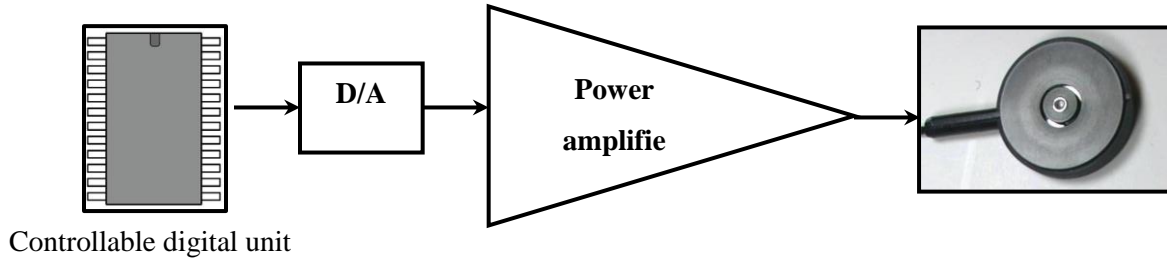
Figure 19: Controlling Hardware Outline

We have provided more details about the different parts of the controlling hardware in the following sections.

3.2 Controllable digital unit

As mentioned previously, the driving hardware requires a controllable digital unit to produce different waveforms. A microcontroller based system is chosen to do this task. A microcontroller is a computer system on a chip. Regarding to Figure 20, a microcontroller contains a processor unit, memory and programmable input/output interfaces. Unlike general purpose computers, microcontrollers are highly specialized for controlling tasks. They require very little power, are very small in size and have a low cost.

An Arduino Mega 1280[61] board was used as the controllable digital unit. The Arduino Mega board takes advantage of an Atmel AVR ATmega1280 [62] microcontroller as its main processing unit. It has 71 digital input/output pins and contains everything needed to operate the microcontroller. It can be connected to a PC via a USB cable and has a number of facilities for communicating with a computer.

The ATmega1280 microntroller provides four hardware UARTs for TTL (5V) serial communication. A serial to USB converter chip on the Arduino board converts one of these srial ports over USB. The drivers provided for the Arduino creates a virtual com port through software on the computer. This feature makes it very simple to provide a serial communication between a PC and the Arduino board.
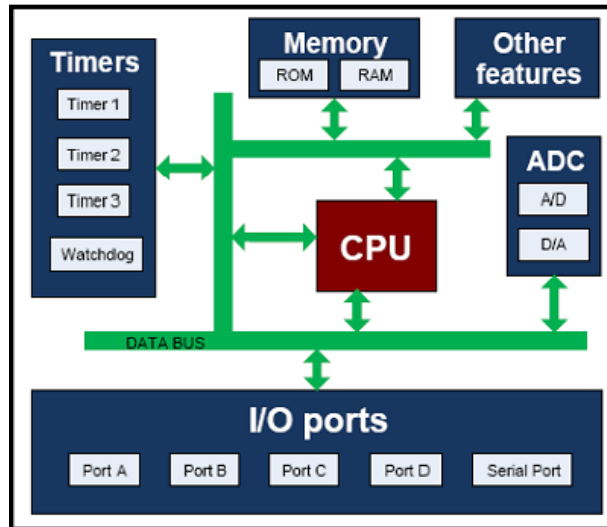
Figure 20: Basic microcontroller architecture
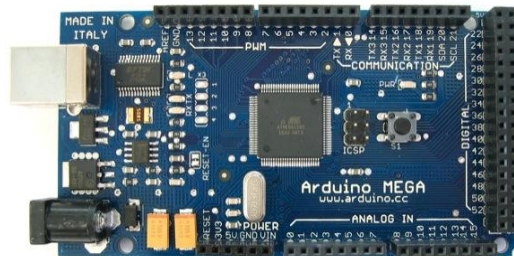
Figure 21: Arduino Mega 1280

3.3 Software

In order to generate desired waveforms, we need to write a suitable program on the Arduino board to perform the task. We took the advantage of a "Direct Digital Synthesize (DDS)" technique to structure the appropriate program. DDS is a frequency synthesize technique used for creating arbitrary waveforms from a single, fixed-frequency reference clock. A simple direct digital synthesizer system is comprised of a precision reference clock, an address counter, a Programmable Read Only Memory (PROM), an output register and a Digital to analogue converter.

In a DDS system, the digital amplitude information that corresponds to a complete cycle of a specific waveform (i.e., sine wave) is stored into the PROM. Therefore the PROM works as a waveform lookup table. The address counter steps through each of the PROM's memory sectors and thus, the contents of

35

the memory are presented to a digital to analogue converter (D/A). Finally, the D/A generates an analogue sine wave in response to the digital input words from the PROM. The frequency of the generated waveform is dependent on the frequency of the reference clock and the waveform step size which is stored in the PROM.

```
┌──────────┐    ┌──────────┐    ┌─────────────────────┐    ┌──────────┐    ┌──────────┐
│ Clock (f_c)│──▶│ Address  │──▶│        PROM         │──▶│  Output  │──▶│ DAC (f_out)│
│          │    │ counter  │    │ (Waveform Lookup table)│    │ register │    │          │
└──────────┘    └──────────┘    └─────────────────────┘    └──────────┘    └──────────┘
```
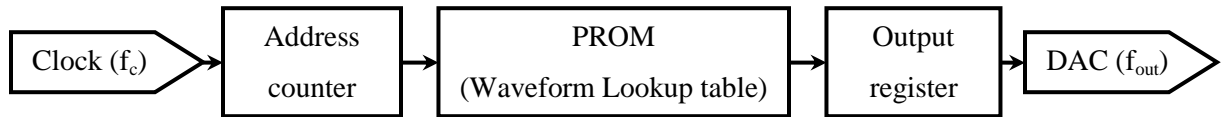
Figure 22: Direct digital synthesizer block diagram

Considering Figure 22, the output frequency can only be changed by varying the frequency of the reference clock or by rewriting the new waveform information into the PROM. Neither of these options supports the high-speed frequency changes for the output.

It is possible to convert this architecture to a fast controllable signal generator by adding a phase accumulator function to the chain. To understand the phase accumulator functionality, consider the digital phase wheel depicted in Figure 23. Each designated point on the phase wheel corresponds to a sector of the PROM. As mentioned previously, the sectors contain digital amplitude information of a specific spot on a cycle of the desired waveform. As the pointer moves around the wheel, the corresponding value of the desired waveform is being generated at the output. One revolution of the pointer around the phase wheel at a constant speed will result in generation of one complete cycle of the desired waveform at the output.

The phase wheel functionality is identical to a look-up table and the phase accumulator is actually a *modulus M counter* that increments its stored number each time it receives a clock pulse. The magnitude of the increment is determined by the value of "M". The value of "M" determines the number of points to skip around the phase wheel. As the value of "M" increases, the frequency of the output waveform increases.

The Arduino board was programmed such that it could provide sine, square, triangle and saw-tooth waveforms at different frequencies (Each waveform has its own look-up table). A serial communication protocol was provided to send the commands from a pc to the Arduino board. We provide detailed description about the communication protocol in section 3.6. The complete program which was provided to program the Arduino board is provided in the appendix A.
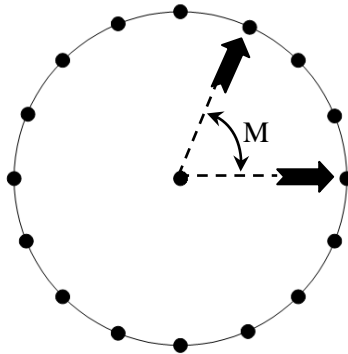
Figure 23: Digital phase wheel. Each designated point on the phase wheel corresponds to a sector of the PROM.

3.4 Digital to Analog Converter

In order to provide proper analogue voltage corresponding to the digital output of the Arduino board, it is necessary to feed the digital output of the board into a digital to analog converter. We used a R-2R resistor ladder network as the DAC unit. A R-2R ladder network is very simple to manufacture and an inexpensive way to perform digital to analog conversion. But, the applied resistors in this structure must be a high precision grade (less than 1%). A basic R-2R ladder network is shown in Figure 24. In this figure, Bit 0 (Least Significant Bit) to Bit 7 (Most Significant Bit) are the outputs of one of the Arduino ports. The resistor ladder network causes the digital bits to be weighted in their contribution to the output voltage. Considering Figure 24, we also took the advantage of a RC circuit to generate better waveforms at the output. In a typical RC circuit, the capacitor discharges its stored energy through the resistor and prevents the sudden changes of the voltage at the output. Therefore, using a RC circuit will result in creation of a smoother waveform at the output.

3.5 Amplifier

The DAC output signal cannot provide enough current for activating a C2 tactor. Hence, this signal cannot be directly fed to a tactor. An amplifier can be utilized in the structure of the driving hardware in order to provide the required current. Furthermore, an amplifier makes it possible to have different levels of amplitude for the output driving signals. The maximum suggested electrical current to activate a C2 tacor is 500mA [60]. Therefore, we need to choose an operational amplifier which is capable of providing

at least 500 mA at its output. The BURR-BROWN OPA547 [63] (High-voltage and high-current operational amplifier) was chosen to perform this task.
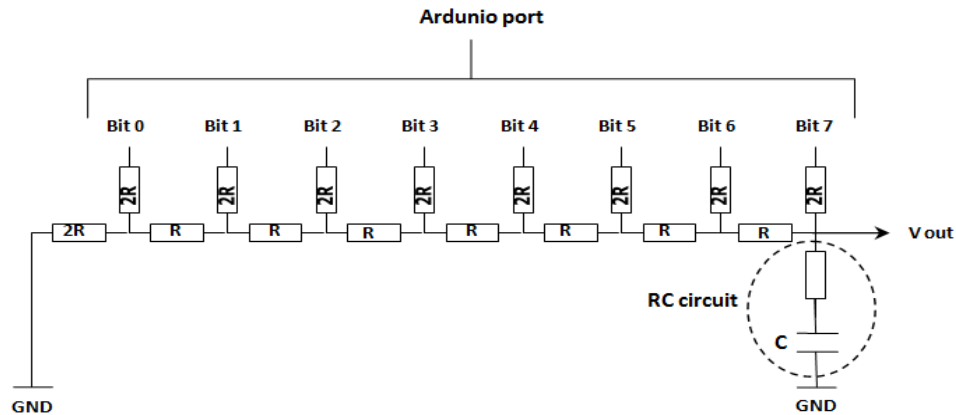
Figure 24: A digital to analogue converter comprised of a R-2R resistor ladder network and a RC circuit. Bit 0 to Bit 7 are the outputs of one of the Arduino ports.

In order to provide different levels of amplitude, we decided to provide 4 different resistors on the negative feedback circuit of the op-amp. We used the FAIRCHILD CD4066BCN [64] analogue switch to select proper feedback resistors for providing different amplitudes at the op-amp's output. The analogue switch was controlled through the Arduino board.

$$Av = \frac{V\ out}{V\ in} = -\frac{R_2}{R_1}$$
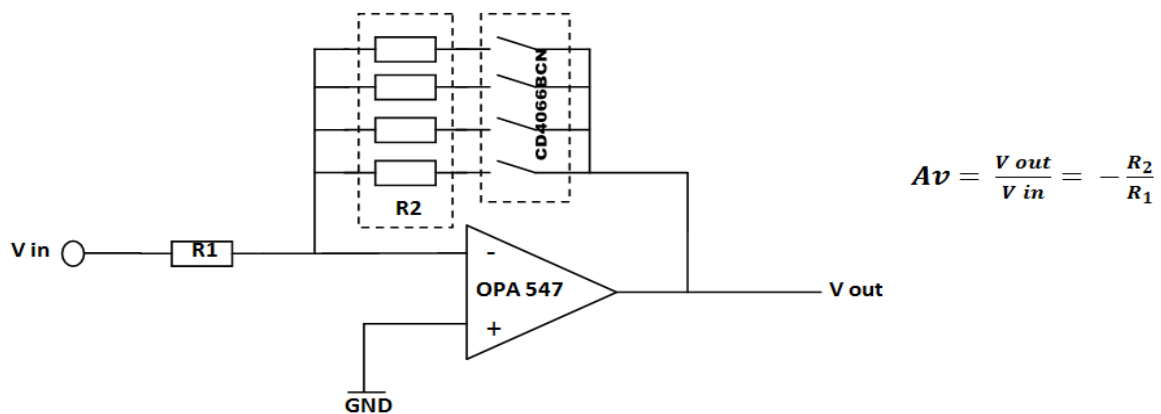
Figure 25: Amplifier circuit schematics. In order to provide different levels of amplitude, 4 different resistors placed on the negative feedback circuit of the op-amp. A FAIRCHILD CD4066BCN [66] analogue switch is used to select proper feedback resistors for providing different amplitudes at the op-amp's output. 38

The electrical resistance of the C2 tactors should be equal to 7 ohms according to the C2 Tactor datasheet [59]. We measured the electrical resistance of the C2 Tactors that we wanted to use, and they were between 8.9 to 9.1 ohms. This value was not consistent with the information mentioned in the datasheet. Therefore, in the design of our driving hardware we considered the electrical resistance of the C2 Tactor equal to 9 ohms.

3.6 Communication Protocol

As mentioned previously, the Arduino board is capable of being connected to a PC through a virtual serial port. Serial communication between the Arduino board and a PC makes it possible to transmit different commands to the driving hardware. We provided a comprehensive communication protocol in order to control the hardware and produce desired driving signals.

Port name	Waveform	Amplitude level	Frequency

Figure 26: The communication protocol structure. Each entry is an ASCII character.

As can be seen from Figure 26, the communication protocol has 4 main entries. Each entry is an ASCII character. An ASCII character is an 8 bit encoding scheme. Therefore, in our communication protocol each communication message has 32 bit length. The protocol is documented in table 1.

The fabricated hardware is capable of providing 5 different signals at its output channels. Generated signals can be different in terms of waveform, amplitude and frequency. It is possible to control the output signal parameters through the communication protocol. Considering Figure 26, the first part of the communication protocol determines the name of the port which is needed to be activated and controlled. The Arduino board has 8 different ports and we designed the hardware such that we can use 5 of these ports to provide 5 different driving signals. The second part of the communication protocol determines the desired shape of the driving signal. The output voltage level and the frequency of the driving signals can be set through the third and fourth parts of the communication protocol respectively.

Table 2: Communication protocol contents

Protocol part	Possible choices and relevant descriptions
Port name	- A: Choose port A to activate - C: Choose port C to activate - F: Choose port F to activate - K: Choose port K to activate - L: Choose port L to activate
Waveform	- a: Choose sine wave - b: Choose triangle wave - c: Choose saw-tooth wave - d: Choose square wave
Amplitude level	- 1: Output signal amplitude equal to 3 volts - 2: Output signal amplitude equal to 3.5 volts 3 - 4: Output signal amplitude equal to 4 volts - Output signal amplitude equal to 4.5 volts
Frequency	- Any number between 0 to 999

As an example, the "Fa2400" command produces a 400Hz sine wave with the amplitude of 3.5 volts will be generated at the port F.

3.7 Hardware Design Summary

Vibrotactor displays are usually comprised of vibratory stimulators which are arranged in a specific formation based on the application of the display. We used the EAI`s C2 Tactor as the vibratory stimulator for the tactile vest. Different tactile parameters can be manipulated to present different messages in vibrotactile displays. Therefore, we designed and fabricated a controller hardware which is

capable of providing different electrical signals with different waveforms, frequencies and amplitudes for tactor activation. The driving hardware benefits from a microcontroller board which can be connected to any PC and can be easily controlled through a serial communication line. Considering C2 tactors are relatively power consuming objects, an operational amplifier which is capable of providing enough current to run a C2 tactor is designated in the structure of the controlling hardware.

Now we have the required hardware to activate C2 tactors, we are interested in analyzing quantitative properties of C2 tactors. In the next chapter we have provided detailed descriptions about the experiments that we run in order to evaluate and investigate the properties of C2 tactors.

Chapter 4
Quantitative Analysis of C2 Tactors

One of the vibrotactile stimulators that have been used in many studies is EAI's C2 Tactor [59]. The C2 Tactor is a miniature vibrator which is designed to be used in vibrotactor displays. Cholewaik et al. investigated the ability of participants in localizing vibratory stimuli around the torso in a study. This was done by utilizing wearable tactor belts which were comprised of C2 Tactors [16]. In another study by Brown et al. the effectiveness of tactons (tactile replication of icons or earcons) were investigated. The tactons were created through a C2 tactor in that study [4]. As mentioned previously, in order to enhance the UAV operators performance we also intend to develop a tactor vest comprised of arrays of C2 Tactors.

The sense of touch is a unique communication channel and vibrotactile displays transfer information by presenting vibrations through this channel. There are five basic vibrotactile parameters which can be manipulated to structure tactile messages in tactile displays [38], [53]. Amplitude, frequency, waveform, duration and location of the stimuli are the primary vibrotactile parameters. According to the datasheet of the C2 Tactor (see appendix A) [59], recommended driving signal for this vibrotactor is a 250 Hz sine wave at 350 mA. But a C2 Tactor can also be driven through electrical signals which are different from the recommended driving signal in terms of waveform, amplitude and frequency. The spec sheet of the C2 tactor is not informative about the responses of this tactor when it is being activated through an electrical signal which is different from the recommended driving signal.

Masking effects are one of the pitfalls in development of vibrotactile interfaces. Masking occurs when two stimuli are presented close to each other in space or time and decrease the detectability of each other [14]. Spatial masking occurs when two stimuli are presented to two distinct locations at different or overlapping times [38], [14]. It is possible to reduce the amount of spatial masking by increasing the distance between stimulated sites in a tactile interface [14], [56]. According to the datasheet of the C2 Tactor, this vibrotactor is designed such that it can be capable of providing a point-like stimulation due to the design of the structure of this tactor [65]. But, the spec sheet of the C2 Tactor did not express that how effective the C2 Tactor's structure is in prevention of the spread of the vibrations and surface waves to adjacent locations. There is not enough information available in the datasheet about the ability of the C2 Tactor in overcoming the masking effects.

Because of the growing application of C2 Tactors in different studies and interfaces, and also because of its special structure, we decided to use this tactor in our tactor vest. We executed a series of experiments investigating the responses of a C2 Tactor when driven through electrical signals which are different from the recommended driving signal stated in the C2 Tactor's datasheet. Driving signals were different in terms of waveform, amplitude and frequency. We have also examined effectiveness of the C2 Tactor's structure in prevention of masking effects.

This section is organized as follows: In section 4.1, the apparatus, the objective and the methodology of the experiments are expressed. In section 4.2 the results of the experiments are provided and discussed and finally we have provided the concluding remarks in section 4.3.

4.1 Method

4.1.1 Apparatus

The apparatus of the experiments included three main parts; a C2 Tactor to provide vibrations, a piece of gel which was molded such that it can replicate the human skin in terms of stiffness and finally an vibration sensor for measuring the intensity of vibrations. We provided detailed description about each part in the following sections.

4.1.1.1 C2 Tactor

Considering Figure 27, A C2 Tactor is a miniature vibrotactor transducer comprised of a moving contactor and a rigid surround. The moving contactor oscillates perpendicular to the skin when an electrical signal is applied. The weight of this tactor is 17 grams. In our experiments, a C2 Tactor was attached to a piece of gel using double side tape. The tape was attached to the tactor such that the tactor's contactor could vibrate without restraint while still being firmly attached to the gel. The thickness of the gel and the double side tape were 15 and 0.01 mm respectively.

Figure 27: A C2 Tactor

4.1.1.2 Gel

A gel was molded from a liquid silicone rubber (Smooth-on Moldmax 10A) such that its stiffness was equal to *shore* 10A. *Shore* is one of the several measurement units used for hardness of materials. Agache et al. [66] investigated the mechanical properties of the human skin. They found that the skin *Young's modulus* is close to 0.42 MPa in young individuals. *Young's modulus* is also a measurement unit used for the stiffness of elastic materials. There is a relation between the Shore hardness and the Young's modulus for elastomers which was derived by Gent [67], as shown in equation (2).

$$E = \frac{0.0981(56 + 7.66S)}{0.137505(254 - 2.54S)}$$

(2)

Where *E* is the *Young's modulus* in MPa, and *S* is the *shore* hardness. By substituting the human skin *Young's modulus* from Agache's study into the equation 1, we found that human skin hardness is equal to *shore* 10.21A which is very close to the stiffness of the molded gel.

4.1.1.3 Vibration Sensor/Accelerometer

In order to measure the vibrations produced by the vibrotactor, a miniature and lightweight vibration sensor/accelerometer were utilized (PCB PIEZOTRONICS vibration sensor model 352C22). The weight of the sensor was 0.5 gram. The output of the vibration sensor was fed to a signal conditioner (PCB PIEZOTRONICS signal conditioner model 480C02) and the output of the signal conditioner was delivered to a data acquisition device (National instruments NI-USB 6216) to capture and record the data. The data acquisition device was connected to a PC through a USB cable.   The intensity of vibrations was measured in terms of m/s^2. The output of the vibration sensor is a voltage signal. According to the datasheet of the vibration sensor, this sensor provides 1 mV signal per 1 m/s^2 of acceleration. Therefore, In order to measure the acceleration magnitude in terms of m/s^2, we just needed to record the peak to peak voltage of the vibration sensor output in terms of mV. Figure 28 indicates the schematics of the electrical setup.

As mentioned previously, we intend to investigate the responses of a C2 Tactor when driven through electrical signals which are different from the recommended driving signal stated in the C2 Tactor's datasheet. The controller hardware which was described in chapter 3 was used to provide the required driving electrical signals.
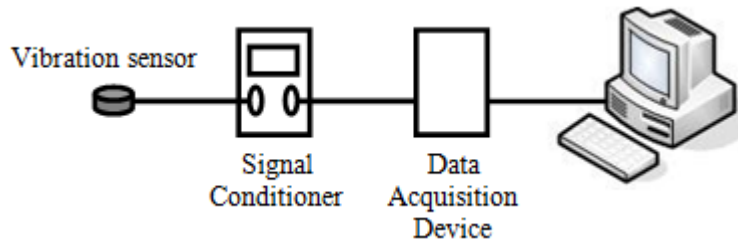
Figure 28: Schematics of the electrical setup

4.1.2 Objectives

Amplitude, frequency and waveform are the three main primary vibrotactile parameters which can be manipulated to structure different tactile messages in tactile displays [38], [53]. The recommended driving signal for C2 Tactor according to its datasheet is a 250 Hz sine wave at 350 mA. But a C2 Tactor can also be activated through electrical signals which are different from the recommended driving signal in terms of waveform, amplitude and frequency.

Changes in the intensity of vibration can be a very useful parameter to encode information in vibrotactile displays [4]. For example, the urgency of a message can be represented by presenting vibrations with different intensities to the operator's skin. Therefore, it is important to know the potential of the C2 Tactor in providing different levels of vibrations. We executed a series of experiments to investigate the responses of a C2 Tactor when it is being driven through electrical signals which are different from the recommended driving signal. Our experimental goals can be summarized as follows:

1- To measure the intensity of the vibrations produced by the C2 Tactor when it is being driven with electrical signals which are different in terms of waveform, frequency or amplitude.

2- To know the range of the intensity of the vibrations that a C2 Tactor can produce when it is being driven with electrical signals which are different in terms of waveform, frequency or amplitude.

3- To investigate the effectiveness of the C2 Tactor's rigid surround in blocking the spread of the vibrations and surface waves to adjacent locations and its capability in prevention of the masking effects.

4.1.3 Procedures

As mentioned previously, we attached the C2 Tactor to the surface of the gel. Three experiments were conducted to examine the objectives. In the first experiment, the frequency and the amplitude of the

45

driving signals did not change. The frequency of the driving signal was 250Hz and its amplitude was 3 volts. We only changed the waveform of the driving signals in this part. First, we attached the tactor to the contactor (the vibrating element of the C2 Tactor) and then we drove the tactor using sinusoidal, square, triangle and saw-tooth waveforms. The intensity of vibration for each of the waveforms were measured and recorded independently. Next, we placed the vibration sensor 0.5, 1.5, and 3 cm away from the external boundary of the C2 Tactor and repeated the measurements described above.

The same procedure was used for the second experiment. The only difference was that we kept the waveform and the amplitude of the driving signal fixed and we only changed the frequency of the driving signals at this part. The waveform of the driving signal was a sine wave and the amplitude was 3 volts. We varied the frequency between 50 – 450Hz with 25 Hz intervals.

For the third experiment we changed the amplitude of the driving signals while keeping the applied waveform and frequency constant. The applied amplitude levels were 3, 3.5, 4 and 4.5 volts. The same procedure as part one and two were followed. The applied waveform was the sine wave and the frequency was 250Hz.

(a)   **(b)**

Figure 29: (a) Accelerometer attached to the contactor using a lightweight (0.5 gr) plastic screw, (b) accelerometer attached to the surface of the gel, 3 cm away from the external boundary of the tactor.

Overall, we had four different positions for the placement of the vibration sensor; *ontop of the contactor* itself, as well as *0.5 cm*, *1.5 cm position* and *3 cm position* from the external boundary of the tactor.

4.2 Results

Figure 30 indicates the results of the first experiment. The recommended waveform for activating a C2 Tactor is mentioned to be a sine wave according to the C2 Tactor's datasheet. But, the results of our first

experiment revealed that the intensity of vibration achieved its highest level when the C2 Tactor was being driven by a square wave signal, and it reached its minimum intensity when a saw-tooth waveform was applied. Sine wave and triangle wave signals had the second and the third most intense vibrations respectively. Saw-tooth and triangle waves produced approximately the same levels of vibration intensity. Overall, we can conclude that when using different waveforms, there is not a huge variation between the different levels of vibration. This result implies that it is not possible to produce many distinguishable levels of vibration through the use of different waveforms. Referring to Figure 30, it is obvious that the intensity of vibration was significantly attenuated when vibration sensor was moved from the *contactor position* to *0.5 cm position*. This result demonstrates the fact that the rigid surround effectively blocked the spread of the surface waves.

Figure 30: Intensity of vibration measured for the first part of the experiments. The vibration sensor was located on the contactor, 0.5 cm away the tactor, 1.5 cm away from the tactor and 3 cm away from the tactor. Driving signals were different in terms of waveform.

The recommended frequency of the driving signal of a C2 Tactor is stated to be 250 Hz in the C2 Tactor's spec sheet. There is not enough information about the quality of the vibrations produced by a C2 Tactor when it is being driven through signals at different frequency ranges. The results of the second experiment are illustrated in Figure 31. It can be seen that the C2 Tactor generates more intense vibrations

when the applied frequency is between 250 – 450 Hz. The vibration reaches its peak intensity at the frequency of 325 Hz. However the optimal frequency range of the C2 Tactor is within the optimal sensitivity range of the human skin to vibration which is reported to be between 150 to 300 Hz [31]. This fact makes a C2 Tactor a proper device to be utilized in vibrotactile displays. Considering figure 6, there is a vast range of vibration intensities covered by signals with different frequencies. Therefore, we can deduce that it is possible to achieve discernible levels of vibration by applying driving signals with different frequencies using a C2 Tactor. Similarly to the first experiment, the second experiment's results show that the rigid surround works effectively to prevent the spread of the waveform on the surface of the skin. As can be seen from the Figure 31, the vibration intensity drastically dropped off as we moved from the *contactor position* to *0.5 cm position*. This rate of drop-off decreases as we move further away from the tactor. For example, the surface wave dissipation from *1.5 cm position* to *3 cm positions* is almost trivial.
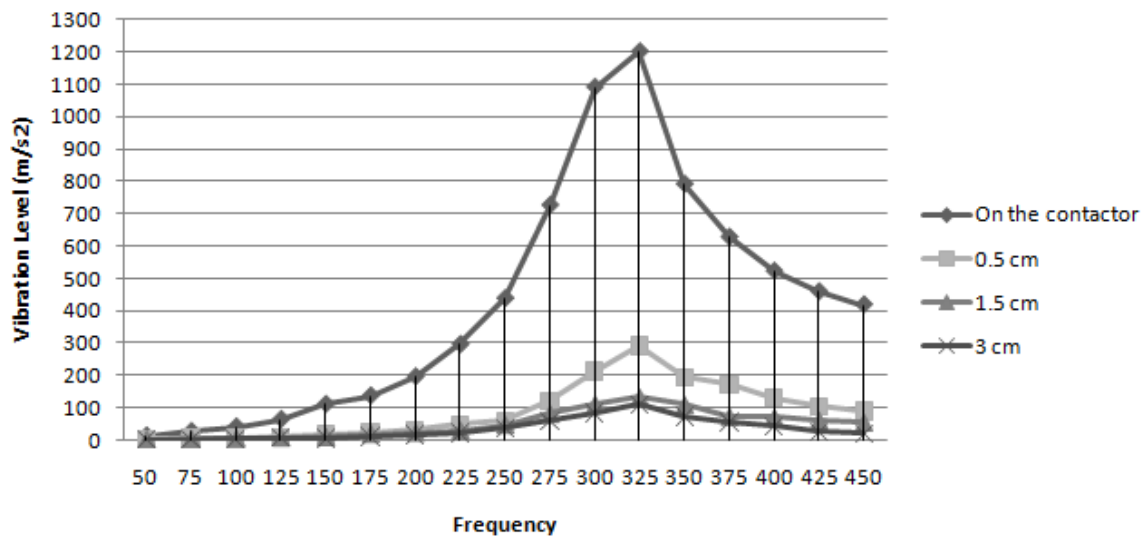
Figure 31: Intensity of vibration measured for the second part of the experiments. The vibration sensor was located on the contactor, 0.5 cm away the tactor, 1.5 cm away from the tactor and 3 cm away from the tactor. Driving signals were different in terms of frequency.

The recommended amplitude for driving a C2 Tactor is 3 volts according to this tactor's datasheet. The datasheet is not informative about the possible intensity levels of vibrations generated by a C2 Tactor when it is being activated through electrical signals which are different in voltage levels. The outcome of the third experiment is provided in Figure 32. As can be seen from the bars, there is approximately a

linear increase in the vibration intensity levels as we increased the amplitude of the driving signals, but the rate of the increment is not considerable. With regards to the results, driving the C2 Tactor with different amplitudes in order to provide discernable levels of vibrations is not suggested. Moreover, the limited electrical properties of the C2 Tactor confined us for applying driving signals with higher amplitudes. Using higher voltage levels for activating a C2 Tactor may results in damage to these miniature tactors. Considering Figure 32, by comparing the results of the *on contactor* and *out of tactor positions* (*0.5 cm*, *1.5 cm* and *3 cm* away from the external boundary of the tactor) we can conclude that the vibration intensity at the *out of tactor positions* are approximately one tenth of the vibration intensity at the *on top of the contactor* position. It is obvious that the rigid surround has largely attenuated propagation of the surface waves.
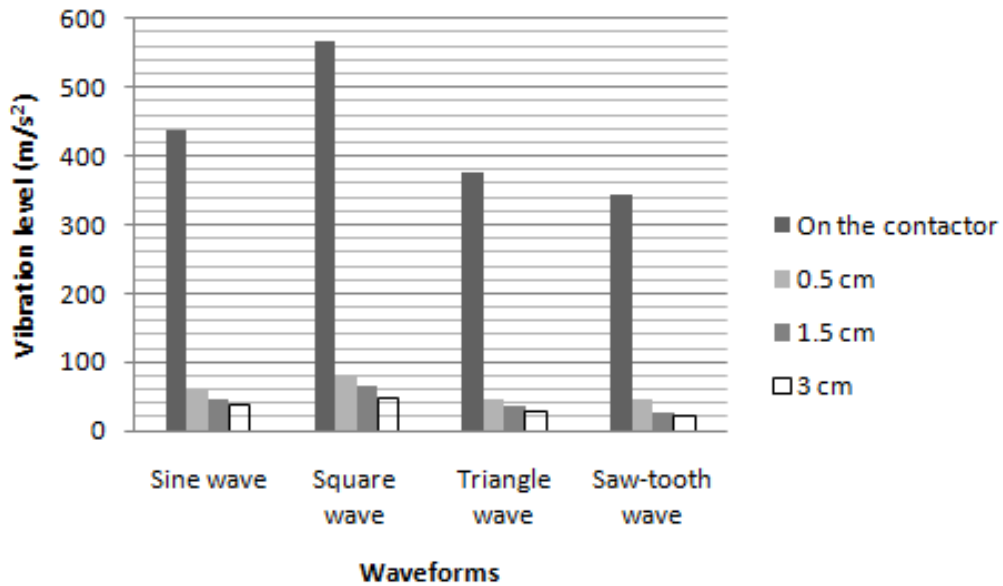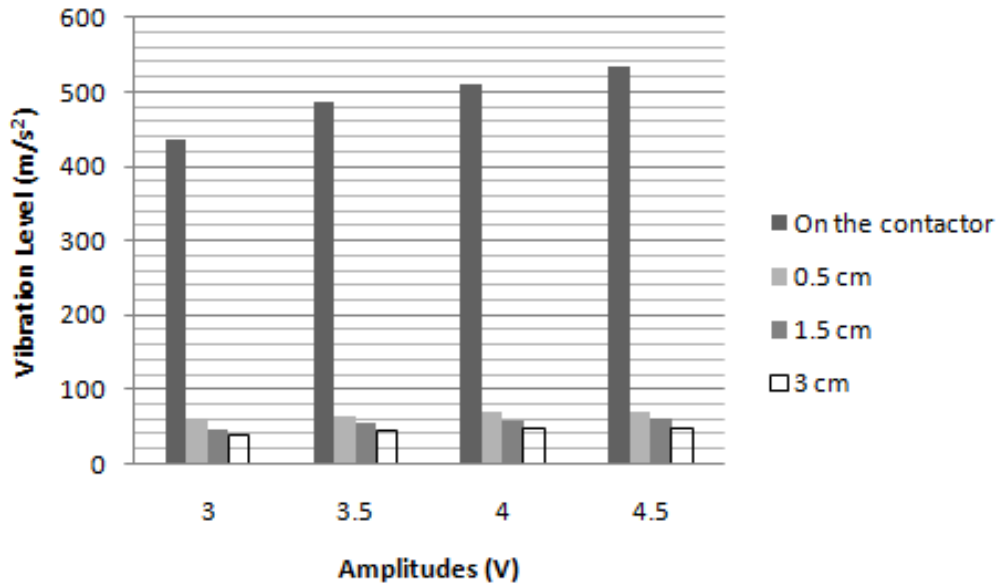

Figure 32: Intensity of vibration measured for the third part of the experiments. The vibration sensor was located on the contactor, 0.5 cm away from the tactor, 1.5 cm away from the tactor and 3 cm away from the tactor. Driving signals were different in terms of amplitude.

4.3 Conclusions and Recommendations

C2 Tactor is one of the vibrotactors which has been applied in several studies and projects. Despite the growing application of this tactor in the design and fabrication of tactile interfaces, unfortunately there is not enough information about the quality and the intensity of the vibrations that this device can generate.

Amplitude, frequency and waveform of the driving signals are the three main vibrotactile parameters which can be manipulated to code different tactile messages in vibrotactile displays. We have executed a series of experiments to find out the range of the intensity of the vibrations that a C2 Tactor can produce when it is being driven with electrical signals which are different in terms of waveform, frequency or amplitude. Results of our experiments revealed that although the recommended waveform for activating a C2 Tactor is a sine wave according to its datasheet, but a C2 Tactor can provide more intense vibrations when it is being fed with a square wave signal. . Overall results revealed that there is not a huge variation between the different levels of vibration when we activate a C2 Tactor using different waveforms.

The recommended frequency of the driving signal of a C2 Tactor is stated to be 250 Hz in the C2 Tactor's spec sheet. The vibration productivity of the C2 Tactor was found to be between 250-450 Hz with its peak at 325 Hz. The optimal frequency range of the C2 Tactor is within the optimal sensitivity range of the human skin to vibration. There was a vast range of vibration intensities covered by signals with different frequencies. Therefore, we can deduce that it is possible to achieve discernible levels of vibration by applying driving signals with different frequencies using a C2 Tactor.

There was a linear improvement in the vibration intensity levels as we increased the amplitude of the driving signals, but the pace of the increment was not considerable. Therefore, in vibrotactile displays, driving the C2 Tactor with different amplitudes in order to generate distinguishable levels of vibrations are not suggested.

Masking effects are one of the challenging issues in development of vibrotactile interfaces. In the spec sheet of the C2 tactor, it is mentioned that this tactor is capable of providing a point-like stimulation due to its structure. But, there are not enough descriptions about the capability of the C2 Tactor in reducing the masking effects. The results of our experiments demonstrated that the C2 Tactor can provide a point-like vibration and be a reliable object to reduce spatial masking effects. The moving contactor of this transducer is surrounded with a passive housing which is very effective in prevention of spread of vibrations to the adjacent locations. Therefore, one of the important properties of the C2 Tactor which makes this device a reliable element to be used in a tactile display is its unique structure.

Considering the outcomes of the experiments we have executed so far, and using the available guidelines for the design of vibrotactile displays, we have proposed some methods for displaying flight dynamics

50

(Roll, Pitch and Yaw) to the torso of the operators through the tactor vest. We explain these display methods in the next chapter.

Chapter 5

Proposed method for displaying flight dynamics parameters using the tactor vest

5.1 Introduction

One of the critical variables that UAV operators are responsible for monitoring during the take-off, cruise, and landing phases flights is the orientation of the UAV. Considering Figure 33, a UAV's attitude is composed of its roll, pitch, and yaw, and any deviations from the UAV's proposed path may lead to an inability for the UAV to land safely. Roll, pitch, and yaw are all spatial variables, and deviations in any of these dimensions could easily be shown using intuitive spatial representations on the tactile vest. Based on our findings regarding the perceptual factors from the past studies (Chapter 1) and C2 Tactor performance (Our experiments and C2 Tactor datasheet) we intend to provide some proposals regarding the presentation of the intensity of a UAV's flight dynamics parameters through the tactor vest. Our proposed methods for displaying roll, pitch, and yaw information were designed to provide an intuitive feeling of what these attitude deviations may feel like on a pilot's body.
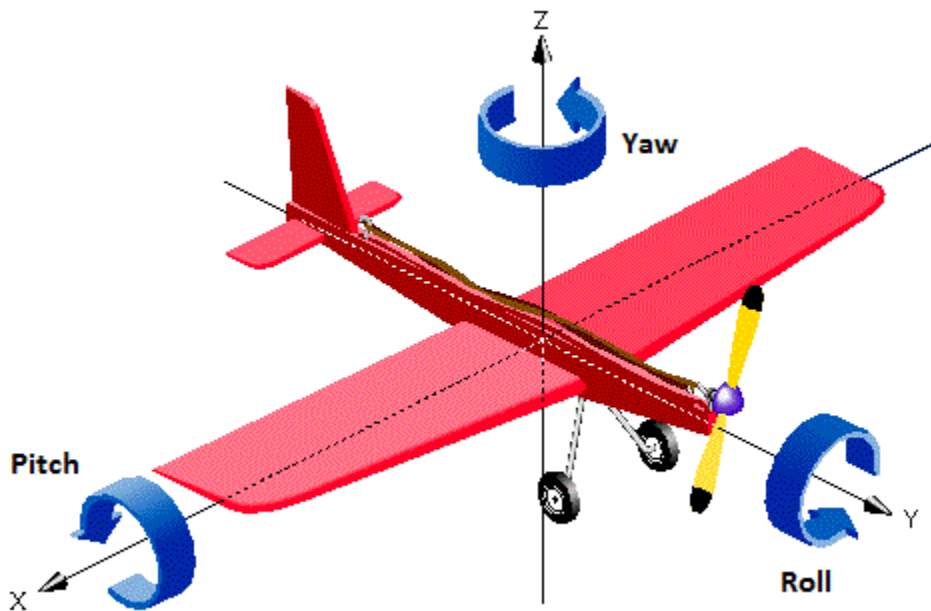
Figure 33: Visual presentation of a cockpit's flight dynamics parameters

Four different types of displays were developed to show attitude deviations: roll, pitch, yaw, and a combined attitude deviation measure. For the individual roll, pitch, and yaw displays, it was important to show both the magnitude of the deviation and the direction of the deviation. For the combined attitude deviation measure, magnitude was determined to be the sole factor which was important to display.

As mentioned in the chapter 1, tactile patterns and perceptions of apparent movement can be generated by sequentially activating a series of vibrotactors placed on the skin[47]. Resulting patterns can be used to intuitively present information regarding orientation or direction of external events. Given the success of such patterns, we feel that patterns could also be used to show attitude information to UAV controllers. We believe using tactile patterns should reduce the amount of error and processing time for understanding the UAV situation by the operators.

It should be mentioned that this chapter of the thesis was first written for a Defence Research and Development Canada (DRDC) report to support the Joint Unmanned Aerial Vehicle Surveillance Target Acquisition System (JUSTAS) project [68]. These materials were prepared under a government of Canada contract and are under crown copyright.

5.1.1 Pattern Display vs. Symbolic Display

It may be possible to display information through tactile symbols. However, little research has been conducted on how efficiently individuals are able to differentiate between various symbols created with tactors [53]. Although letter recognition in Yanagida et al. [52] experiments was relatively successful (87% correct letter or number recognition), it should be noted, however, that in the Yanagida et al. experiments, participants were not asked to perform any additional tasks and that in high workload conditions accuracy may decline.

In another study by McKinley et al. [69] three different tactons were used to present enemy, unknown and friendly aircrafts to pilots. The location of the tactons on the vest indicated the spatial location of the target aircrafts relative to the subject's aircraft. The results of this study indicated that the differentiation between different tactons was not easy. Also the individual's familiarity with the displayed set of symbols may also affect the accuracy of the pattern recognition process. Thus, the size of the symbol set and the training given to operators become critical factors.

Regarding the facts mentioned above it seems using tactile patterns for displaying information through the tactor vest can help to execute our goal.

Spatial acuity for vibration is relatively uniform over the trunk and is approximately 2–3cm for vibrotactile stimuli. This acuity is better for horizontally oriented arrays located in line with the spine and navel and is approximately 1cm in these regions [8]. Therefore, inter-tactor spacing should be at least 3cm for the proposed configurations. The results of our experiments on the C2 Tactor also revealed that the propagation of the surface waves is trivial due to the structure of the C2 Tactor. Hence, 3 cm is an appropriate distance for inter-tactor spacing.

5.2 Proposed Methods for Displaying Roll

The suggested tactor configurations for displaying the angle of the roll are depicted on the Figure 34. The first configuration (a) requires 31 tactors and the second configuration (b) requires 21 tactors. These tactor configurations can be positioned either on the front or the back of the vest.
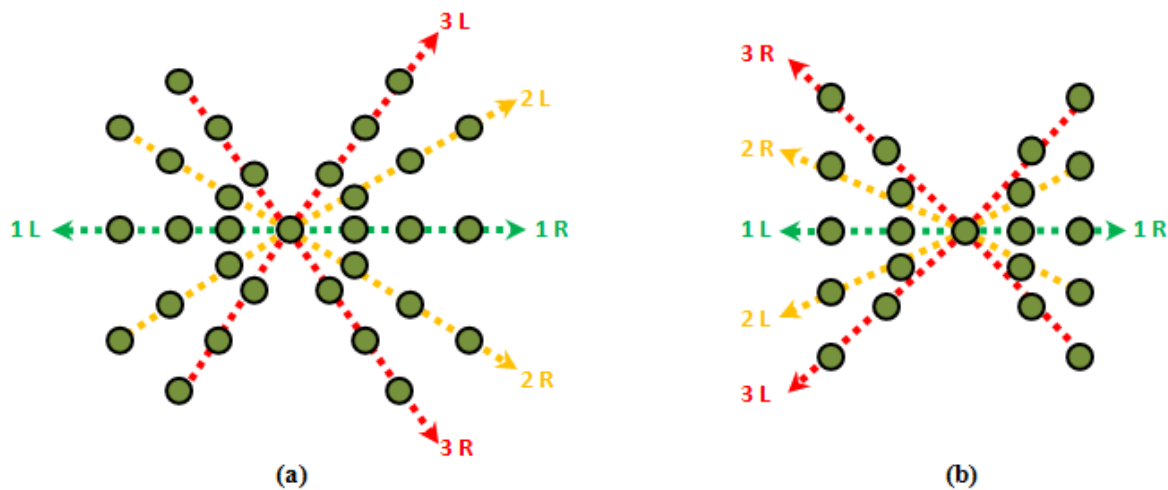
Figure 34: Suggested tactor configuration for roll presentation

Both of these tactor configurations present information through moving tactile patterns. It is possible to present three completely separate levels of roll through the configurations provided above. The mapping of degrees of roll deviation to the different levels is a task that must be accomplished at a later stage. The first level of roll deviation is presented by activating the tactors located on the green dotted line. For example if the UAV's roll deviation is less than 20 degrees to the right, we can show this by activating

the tactors aligned on the right side of the green dotted line, indicated by "1 R" Higher levels of roll deviation can be shown by activating the tactors aligned on the yellow and red dotted lines. For example if the UAV's roll deviation is more than 20 and less than 40 degrees to the left, we can show this by simultaneously activating the tactors aligned with the yellow dotted lines designated "2 L."

5.2.1 Tactor Activation Sequence for Displaying Roll

The simultaneous activation of two vibrotactors located close together causes the sensation of only a single point between the two tactors (apparent location). This point shifts continuously toward the vibration with higher intensity [49]. We can apply this phenomenon to our proposed method, to remove the feeling of discrete levels of UAV roll deviation on the tactor vest. For example when UAV's roll changes from **"1 R"** to **"2 R"**, as in Figure 35, tactor activation sequence would be as follow:

1- Reduce the vibration amplitude of the "1 R" tactors from 100% to 50% of their maximum value and increase the vibration amplitude of the "2 R" tactors from 0% to 50% of their maximum value.

2- Reduce the vibration amplitude of the "1 R" tactors from 50% to 0% of their maximum value and increase the vibration amplitude of the "2 R" tactors from 50% to 100% of their maximum value.

By using this activation strategy we can provide sensations of apparent locations between the actual locations of the tactors. This may aid in decreasing the confusion in understanding the UAV's current roll deviation by providing more perceivable levels of roll information.
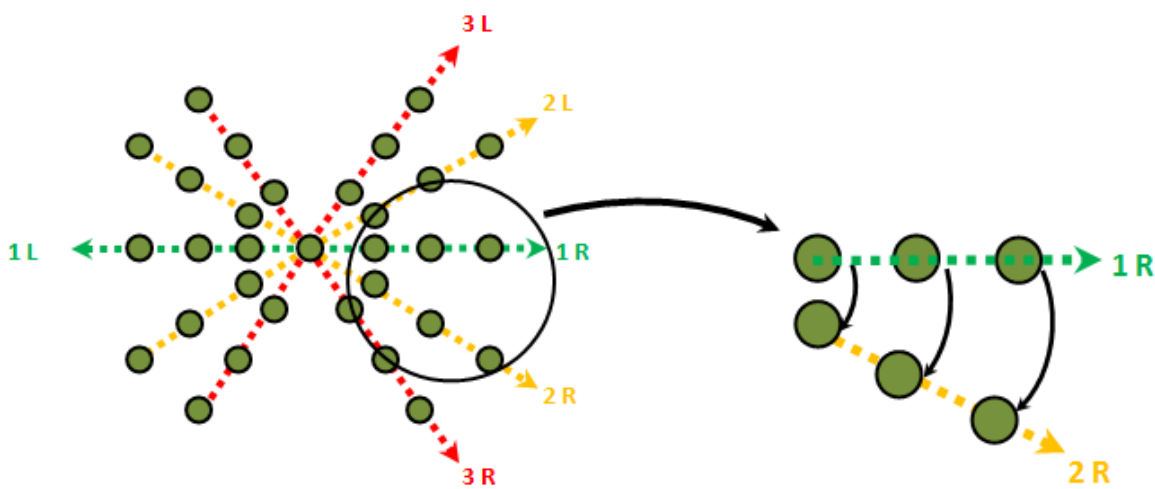
Figure 35: Tactor activation sequence for roll display.

55

5.3 Proposed Method for Displaying Yaw

The effectiveness of a vibrotactile torso display as a countermeasure to spatial disorientation was investigated by Van Erp et al. [45]. In this study, participants wore a vibrotactile display vest which consisted of 24 columns of 2 vibrotactors while seated on a rotating chair. This vibrotactile display was designed to help participants recover from spatial disorientation. The results of this experiment demonstrated that a vibrotactile display can assist operators as they recover from loss of spatial orientation.

Inspired by the Van Erp et al. (2006) experiments, our display indicates the UAV's yaw (heading) deviation using a simple tactor configuration. As shown in Figure 36, a row of tactors, consisting of five C2 tactors, is placed in the frontal region of the tactor vest. The UAV heading can be displayed by sequentially activating the vibrotactors along the observer's chest or abdomen along the horizontal plane. In this method, the vibrotactile signal moves in the same direction of the UAV's yaw deviation. The tactor located on the midsagittal plane of the torso acts as the null point in this configuration.

It should be noted that this display is only activated when the UAV's heading deviates from its desired heading. For example, if the UAV is programmed to travel from Point A to Point B, it has to hold a specific heading. If for any reason (such as turbulence or wind-shear) the UAV's heading deviates from its desired value, the yaw display can be activated to show the intensity of the yaw divergence. This is illustrated in Figure 37.

5.4 Proposed Method for Displaying Pitch

Our suggested configuration for displaying pitch is very similar to the configuration used in the yaw display. As can be seen in Figure 38, this configuration makes use of a vertical column of five C2 tactors in the frontal region of the tactor vest. The UAV pitch can be displayed by sequentially activating the vibrotactors aligned along the observer's midsagittal plane. In this method, the vibrotactile stimuli move in the same direction as the UAV's pitch deviation. The middle tactor (the third of five tactors) acts as the null point in this configuration.
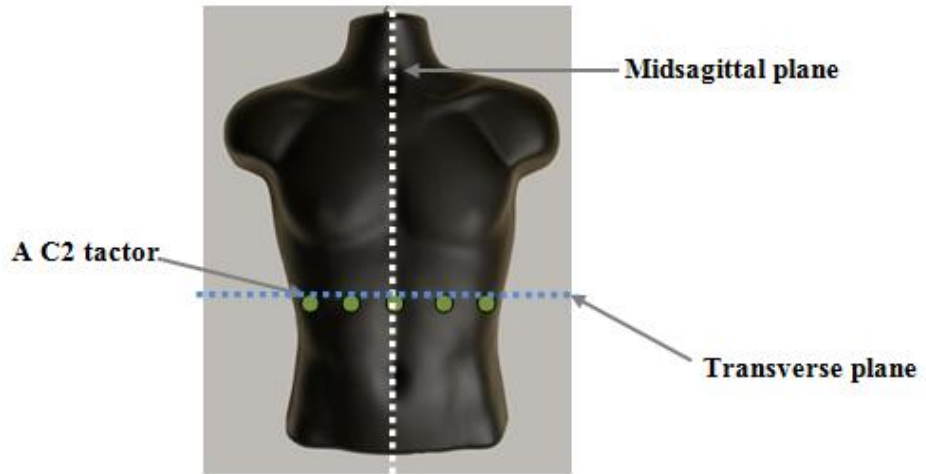
Figure 36: Suggested tactor configuration for yaw presentation.
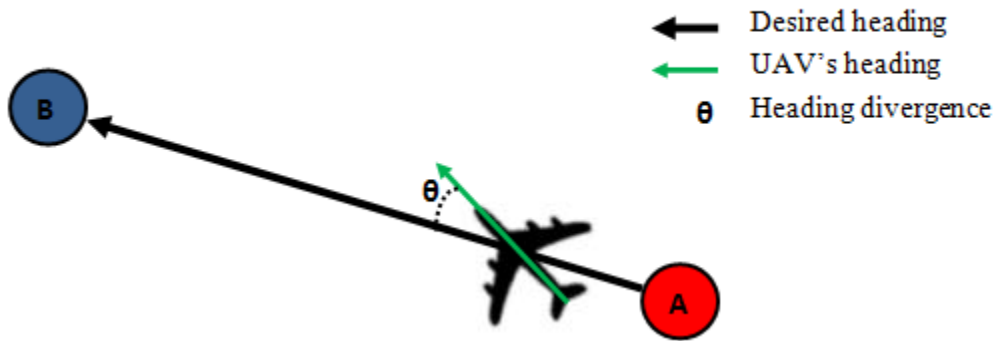
Figure 37: UAV's heading and desired heading.
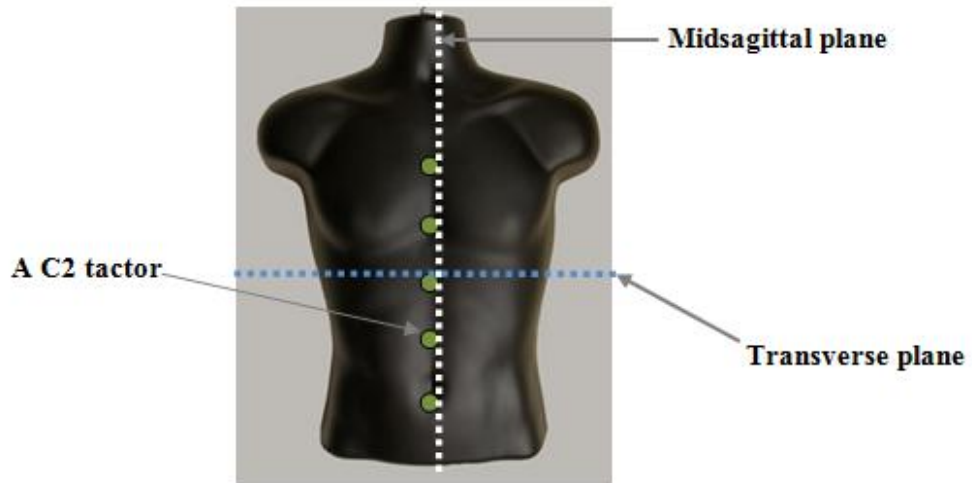
Figure 38: Suggested tactor configuration for pitch presentation.

Similar to the yaw display, this display is only activated when the UAV's pitch angle deviates from its desired pitch angle. For example, during an UAV recovery, the UAV has an ideal glide slope which it attempts to maintain. As shown in Figure 39, if for any reason (such as turbulence or wind shear) the UAV's pitch angle deviates from its desired value, the pitch display can be activated to show the intensity and direction of the pitch angle divergence.

Figure 39: UAV's pitch angle and desired pitch angle.

5.5 Combination of Yaw and Pitch Display to Form Yaw-Pitch Display

In the last few sections we introduced and described the relevant tactor configurations to present yaw and pitch through the tactor vest. We believe that we can combine these configurations to construct a more complex tactor display. We call it a yaw-pitch display.

As Figure 40 shows, the yaw-pitch display would be constructed of a 5×5 tactor matrix. This tactor configuration is capable of showing yaw and pitch intensity concurrently. The intensity of yaw can be presented by activation of tactors along the horizontal axis and the intensity of pitch can be displayed by activation of tactors along the vertical axis. Therefore the yaw intensity would be presented in terms of the distance between the activated tactor and the midsagittal plane of the body, and the pitch angle would be presented in terms of the distance between the activated tactor and the transverse plane of the torso.
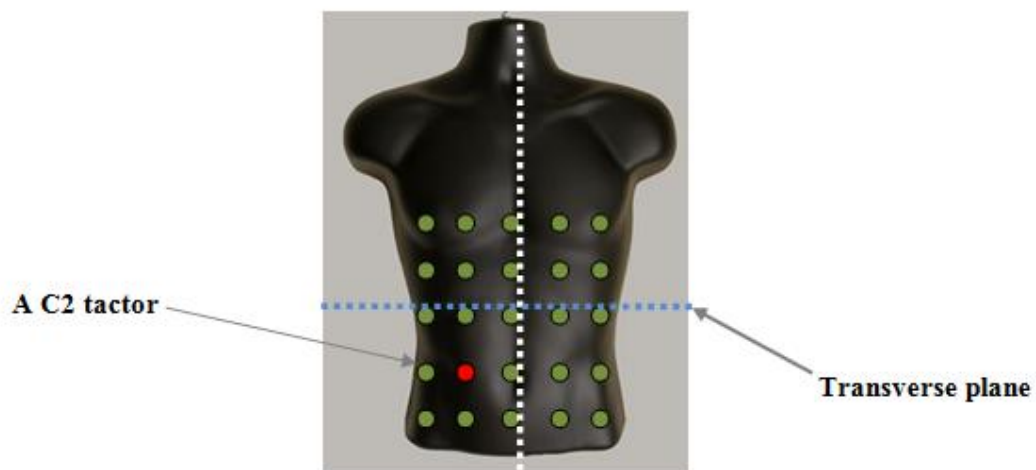
Figure 40: Suggested tactor formation for Pitch-Yaw display.

For instance, if the tactor indicated in red is activated (shown in Figure 2.10), this would represent a situation in which the UAV has a yaw deviation to the right and downwards pitch deviation.

The use of two tactile patterns in combination is one that has not been reported in the literature and this combination may bring to light many interesting questions regarding how efficiently operators can detecting the two patterns concurrently. We feel that the patterns provide information which is sufficiently different and intuitive, that the operator would be able to make use of both displays at once. This should, however, be investigated further.

5.6 Conclusion

In the previous sections we proposed and explored attitude displays that would provide information about flight dynamic parameters that could be presented independently and concurrently. The roll display was designed such that it could be mounted on the back of the vest, while the pitch-yaw displays could be mounted on the front side of the vest. Therefore, it may be possible for UAV operators to perceive the intensity of the roll, pitch, and yaw using the the vibrotactile vest. The use of two tactile patterns at once is one that has not been reported in the current available literature, and there may be many interesting questions about how well operators are at detecting both patterns concurrently.

Human factor issues have major influences on design and application of any vibrotactile display. Therefore we should consider the perceptual factors in pattern generation and coding procedure. Due to the relative infancy of this branch of information presentation, and also the lack of thorough discussion within the scientific community, further experiments are needed to evaluate the performance of the suggested tactile displays. Such experiments should be designed based on *Human Factors Engineering* principles which are out of the scope of this study.

Chapter 6
Conclusions

The sense of touch is one of the most important modalities which human uses to interact with the outside world. It is obvious that a simple tap on a body site can draw our attention to the direction of the stimulant even when we are not paying attention. Hence, stimulation of the skin can be a powerful way to passively convey spatial information. The surface of the body can play an important role in presenting information to operators in situations where their other senses are being used or overloaded.

The majority of research that has attempted to investigate the accuracy and limitations of the sense of touch has typically tended to present stimuli to more sensitive regions of skin, such as hands and finger tips. Although hands may have better discriminative power than the rest of the body parts, most of the current interfaces already require the use of the operator's hands and limbs for control activities. This fact highlights the importance of investigating the potential for using the surface of the torso as an alternative way to convey information.

The main objective of our study was to identify the key findings on how to use tactile technology effectively to design and fabricate a wearable tactile interface. We proposed a tactile display such that it can display the spatial orientation of a UAV to the body of a UAV operator. In order to develop a strong foundation of tactile perception research, we accomplished a comprehensive literature review on tactile perception. The results of the background review are organized in the chapter 1.

Tactile interfaces are comprised of tactors which provide the required vibratory stimuli to construct the tactile messages. We used the C2 Tactor as the vibrating element for our tactile display. Amplitude, frequency, waveform, duration and location of the vibrations are the primary vibrotactile parameters which can be manipulated in order to construct tactile messages in a vibrotactile interface. Hence, a controller hardware is designed and fabricated which is capable of generating electrical signals with different waveforms, frequencies and amplitudes for tactor activation.

Despite the growing application of C2 Tactors in several studies and interfaces, unfortunately there was not enough information about the quality and the intensity of the vibrations that this device can generate. Hence, we executed a series of experiments to examine the C2 Tactor when it is being driven through different electrical signals. The results of our experiments demonstrated that a C2 Tactor can generate more intense vibrations when it is being activated through a square wave signal. In terms of frequency,

the highest vibration intensity can be produced when a C2 tactor is activated through a 325 Hz signal. Experiment results revealed that using different levels of amplitude do not significantly affect the vibration intensity levels generated by a C2 Tactor. The results also proved that a C2 Tactor's structure is very effective in reducing spatial masking effects.

By applying the outcomes of our experiments and using the available guidelines for the design of vibrotactile displays, we proposed some methods for displaying flight dynamics parameters (Roll, Pitch and Yaw) to the torso of the body using the tactor vest. We benefit from spatio-temporal tactile patterns in order to generate the tactile messages in our suggested methods. The use of tactile patterns for displaying complex spatial information has not been reported in the current available literature. Therefore, it is needed to develop a series of experiments to evaluate the efficacy of the suggested display and enhance the design.

REFRENCES

1. *Haptic perception: A tutorial.* **Lederman, S. J., Klatzky, R. L.** 2009, Attention, Perception & Psychophysics, Vol. 71, pp. 1439-1459.

2. *Tactile Information presentation in the cockpit.* **Van Veen, H. A. H. C., Van Erp, J. B. F.** 2000, Haptic Human-Computer Interaction, pp. 174-181.

3. *An instrumentation solution for reducing spatial disorientation mishaps.* **Rupert, A.H.** 2000, IEEE Engineering in Medicine and Biology, Vol. 19, pp. 71-80.

4. *Multidimensional tactons for non-visual information presentation in mobile devices.* **Brown, L. M., Brewster, S.A., Purchase, H. C.** 2006a. Proceedings of eight ACM international conference on Human-Computer Interaction with Mobile Devices and Services. pp. 231-238.

5. *Using spatial vibrotactile cues to direct a driver's visual attention.* **Ho, C. , Tan, H. Z., Spence, C.** 2005, Transportation Research Part F: Traffic Psychology and Behaviour, Vol. 8, pp. 397-412.

6. *A multipurpose tactile vest for astronauts in the international space station.* **Van Erp, J. B. F., Van Venn, H. A. H. C.** 2003. In proceedings of Eurohaptics. pp. 405-408.

7. *Vibrotactile in-vehicle navigation system.* **Van Erp, J. B. F., Van Veen, H. A. H. C.** 2004, Transportation Research Part F: Traffic Psychology and Behaviour, Vol. 7, pp. 247-256.

8. *Waypoint navigation with a vibrotactile waist belt.* **Van Erp, J. B. F., Van Veen, H. A. H. C., Jansen, C., Dobbins, T.** 2005, ACM Transactions on Applied Perception, Vol. 2, pp. 106-117.

9. **Giang, W., Santhakumaran, S., Masnavi, E., Glussich, D., Kline, J., Chui, F., Burns, C., Histon, J., Zelek, J.S.** *Multimodal Interfaces, Literature Review of Ecological Interface Design, Multimodal.* Advanced Interface Design Laboratory, University of Waterloo. Toronto : Defence R&D Canada, 2010.

10. **Kandel, E. R., Schwartz, J. H., Jessel, T. M.** *Principles of Neural Science.* New York : Elsevier Science Publishing Co, 1991.

11. *The psychophysics of tactile perception and its peripheral physiological basis, in pain and touch.* **Greenspan, J. D.,Bolanowski, S.J.** [ed.] L. Kurger. s.l. : Academic Press, 1996.

12. *Sensory and physiological bases of touch.* **Cholewiak, R.W., Collins, A.A.** [ed.] M. A., Schiff, W. Heller. s.l. : Lawrence Erlbaum Associates: Hillsdale, N. J, 1991, In The Psychology of Touch, pp. 23-60.

13. *Tactile Displays: a short overview and recent developments.* **Chouvardas, V. G., Miliou, A. N., Hatalis, M. K.** 2005. 5th International Conference on Technology and Automation. pp. 246-251.

14. **Cheung, B., Van Erp, J.B.F., & Cholewiak, R.W.(2008).** *Anatomical, neurophysiological and perceptual issues of tactile perception.In J.B.F. van Erp & B.P.Self (Eds), Tactile displays for orientation, navigation and communication in air, sea and land enviroments (Report No. TR-HFM-122, p.2-1 - 2-18).* France : Neully-sur-Seine Codex, North Atlantic Treaty Organization, Research and Technology Organization.

15. **Sherrick, C.E., Cholewiak, R.W.** Cutaneous sensitivity. [ed.] K. R., Kaufman, L., Thomas, J. P. Boff. *in Handbook of perception and human performance.* New York : John Wiley and sons, 1986, pp. 12-1 -- 12-58.

16. *Vibrotactile localization on the abdomen: Effects of place and space.* **Cholewiak, R. W., Brill, J. C., Schwab, A.** 2004, Perception & Psychophysics, Vol. 66, pp. 970-987.

17. *Vibrotactile spatial acuity on the torso: effects of location and timing parameters.* **Van Erp, J. B. F.** 2005b. Proceedings of the First Joint Eurohaptics Conference and Symposium on Haptic Interfaces for Virtual Environment and Teleoperator Systems. pp. 80-85.

18. *Vibrotactile localization on the arm: Effects of place, space, and age.* **Cholewiak, R. W., Collins, A. A.** s.l. : 65, 2003, Perception & Psychophysics, pp. 1058–1077.

19. *Attentional and perceptual limitations in processing sequentially presented vibrotactile targets.* **Hillstrom, A. P., Shapiro, K., Spence, C.** 2002, Perception & Psychophysics, Vol. 64, pp. 1068–1082.

20. *The Body Surface as a Communication System: The State of the Art after 50 Years.* **Gallace, A., Tan, H. Z., Spence, C.** 2007, Teleoperators and Virtual Environments, Vol. 16, pp. 657-676.

21. *Trunk orientation as the determining factor of the "contralateral" deficit in the neglect syndrome and as the physical anchor of the internal representation of body orientation in space.* **Karnath, H. O., Schenkel, P., Fischer, B.** 1991, Brain, Vol. 114, pp. 1997-2014.

22. *Presenting directions with a vibrotactile torso Display.* **Van Erp, J. B. F.** 2005a, Ergonomics, Vol. 48, pp. 302 -313.

23. *The nature of pressure adaptation.* **Nafe, J. P., Wagoner, K. S.** 1941, Journal of General Psychology, Vol. 25, pp. 323-351.

24. *The magical number seven, plus or minus two: Some limitations on our capacity for processing information.* **Miller, G. A.** 1956, Psychological Review, Vol. 63, pp. 81-97.

25. *Tactons: Structured tactile messages for non-visual information display.* **Brewster, S. A., & Brown, L. M.** Sydney, Australia : Australian Computer Society, 2004. In Proceedings of the 5th Australasian User Interface Conference. pp. 15-23.

26. *Intensive and extensive aspects of tactile sensitivity as a function of body-part, sex and laterality.* **Weinstein, S.** 1968, The Skin Senses, pp. 195-222.

27. *Optical-to-tactile image conversion for the blind.* **Bliss, J. C., Katcher, M. H., Rogers, C. H., Shepard, R. P.** 1970. IEEE Transactions on Man–Machine Systems. Vols. MMS-11, pp. 58-64.

28. *Vibrating insoles and balance control in elderly people.* **Priplata, A. A., Niemi, J. B., Harry, J. D., Lipsitz, L. A., Collins, J. J.** 2003, Lancet, Vol. 362, pp. 1123-1124.

29. *Acomparison of Tactaid II+ and Tactaid 7 use by adults with a profound hearing impairment.* **Galvin, K. L., Mavrias, G., Moore, A., Cowan, R. S., Blamey, P. J., Clark, G. M.** 1999, Ear and Hearing, Vol. 20, pp. 471–482.

30. **Enginnering Acoustics, Inc.** Enginnering Acoustics Entertainment Products and Technology. [Online] Enginnering Acoustics, INC, 2008. http://www.eaiinfo.com/Entertainment%20Page.htm.

31. *Tactile displays: Guidance for their design and application.* **Jones, L.A., Sarter, N.B.** 1, 2008, Human Factors, Vol. 50, pp. 90-111.

32. *On the vibrational sensitivity in different regions of.* **Wilska, A.** 1954, Acta Physiologica Scandinavica, Vol. 31, pp. 285-289.

33. *Investigation of some parameters of the cutaneous threshold for vibration.* **Verrillo, R.T.** 11, 1962, The Journal of the Acoustical Society of America, Vol. 34, pp. 1768-1773.

34. *Effect of contactor area on the vibrotactile threshold.* **Verrillo, R.T.** 12, 1963, Journal of Acoustical Society of America., Vol. 35, pp. 1962-1966.

35. *Effect of spatial parameters on the vibrotactile threshold.* **Verrillo, R.T.** 4, 1966, Journal of Experimental Psychology, Vol. 71, pp. 570-575.

36. *Vibrotactile frequency for encoding a speech parameter.* **Rothenberg, M., Verrillo, R. T., Zahorian, S. A., Brachman, M. L., Bolanowski, S. J.** 1977, Journal of the Acoustical Society of America, Vol. 62, pp. 1003-1012.

37. *A scale for rate of tactual vibration.* **Sherrick, C. E.** 1, 1985, Journal of the Acoustical Society of America, Vol. 78, pp. 78-83.

38. *Guidelines for the use of vibro-tactile displays in human computer interaction.* **Van Erp, J.B.F.** 2002. Proceedings of Eurohaptics. pp. 18-22.

39. *Information from time-varying vibrotactile stimuli.* **Summers, I. R., Cooper, P. G., Wright, P., Gratton, D. A., Milnes, P., Brown, B. H.** 1997, Journal of the Acoustical Society of America, Vol. 102, pp. 3686-3696.

40. *Difference threshold for intensity of tactile stimuli.* **Craig, J.C.Craig, J.C.** 2, s.l. : Perception & Psychophysics, 1972, Perception and Psychophysics, Vol. 11, pp. 150-152.

41. *Sensation magnitude of vibrotactile stimuli.* **Verrillo, R. T., Fraioli, A. J., & Smith, R. L.** s.l. : Psychonomic Journals Inc, 1969, Perception and Psychophysics, Vol. 6.

42. *Tactile vibration: Change of exponent with frequency.* **Stevens, S. S.** 1968, Perception and Psychophysic, Vol. 3, pp. 223-228.

43. *Perception of short tactile pulses generated by a vibration motor in a mobile phone.* **Kaaresoja, T., & Linjama, J.** Los Alamitos, CA : IEEE Computer Society. In Proceedings of the First Joint Eurohaptics Conference and Symposium on Haptic Interfaces for Virtual Environment and Teleoperator Systems. pp. 471-472.

44. *A First Investigation into the Effectiveness of Tactons.* **Brown, L. M., Brewster, S. A., & Purchase, H. C.** Los Alamitos, CA : IEEE Computer Society, 2005. In Proceedings of the First Joint Eurohaptics Conference and Symposium on Haptic Interfaces for Virtual Environment and Teleoperator Systems. pp. 167-176.

45. *A Tactile Cockpit Instrument Supports the Control of Self-Motion During Spatial Disorientation.* **Van Erp, J. B. F., Groen, E. L., Bos, J. E., Van Veen, H. A. H. C.** 2, 2006, Human factors, Vol. 48, pp. 219-228.

46. *Empirical Studies for Effective Near-Field Haptics in Virtual Environments.* **Lindeman, R. W., & Yanagida, Y.** Los Alamitos, CA : IEEE Computer Society, 2003. In Proceedings of the IEEE Virtual Reality Conference. pp. 287-288.

47. *The generation of vibrotactile patterns on a linear array: Influences of body site, time, and presentation mode.* **Cholewiak, R.W., Collins, A.A.** 6, 2000, Perception and Psychophysics, Vol. 62, pp. 1220-1235.

48. *Cutaneous perception of a track produced by a moving point across the skin.* **Langford, N., Hall, R. J., Monty, R. A.** 1973, Journal of Experimental Psychology, Vol. 97, pp. 59-63.

49. *The localization of low- and high-frequency vibrotactile stimuli.* **Sherrick, C.A., Cholewiak, R.W. & Collins, A.A.** 1, 1990, Journal of the Acoustical Society of America, Vol. 88, pp. 169-178.

50. *Tactile apparent movement: the effects of interstimulus onset interval and stimulus duration.* **Kirman, J.H.** 1, 1974, Perception and Psychophysics, Vol. 15, pp. 1-6.

51. *Tactile display and vibrotactile pattern recognition on the torso.* **Jones, L. A., Lockyer, B., Piateski, E.** 12, 2006, Advanced Robotics, Vol. 20, pp. 1359-1374.

52. *Vibrotactile Letter Reading Using a Low-Resolution Tactor Array.* **Yanagida, Y., Kakita, M., Lindeman, R.W., Kume, Y., Tetsutani, N.** 2004. Proceedings of the 12th International Symposium on Haptic Interfaces for Virtual Environment and Teleoperator Systems, HAPTICS. pp. 400-406.

53. **Self, B.P., Van Erp, J.B.F., Eriksson, L. & Elliott, L.R. .** *Human Factors Issues of Tactile Displays for Military Envirometns.In J. B. F. van Erp & B. P. Self (Eds.) Tactile Displays for Orientation, Navigation and Communication in Air, Sea and Land Environments (Report No. TR-HFM-122).* France : Neuilly-sur-Seine Cedex, North Atlantic Treaty Organization, Research and Technology Organization publication, 2008.

54. *Vibrotactile masking and the persistence of tactual features.* **Craig, J.C., Evans, P.M.** 4, 1987, Perception & Psychophysics, Vol. 42, pp. 309-317.

55. *Vibrotactile masking: effects of stimulus onset asynchrony and stimulus frequency.* **Gescheider, G., Bolanowski, S., & Verrillo, R.** 5, s.l. : The Journal of the Acoustical Society of America, 1989, Vol. 85, pp. 2059-2064. Retrieved from http://www.ncbi.nlm.nih.gov/pubmed/2732386.

56. *Spatial Factors in Vibrotactile Pattern Perception In C. Baber, M. Faint, S. Wall, & A. M. Wing (Eds.).* **Cholewaik, R. W., Collins, A. A., Brill, C. J.** s.l. : Eurohaptics, 2001.

57. *Vibrotactile masking: Effects of one- and two-site stimulation.* **Verrillo, R.T., Gescheider, G.A.** 4, 1983, Perception and Psychophysics, Vol. 33, pp. 379-387.

58. *Vibrotactile difference thresholds for intensity and the effect of a masking stimulus.* **Craig, J. C.** 1, s.l. : Perception & Psychophysics, 1974, Vol. 15, pp. 123-127.

59. **Enginnering Acoustics, INC.** C2 Tactor Datasheet. [Online] 2008. http://www.eaiinfo.com.

60. **Engineering Acousics, INC.** Tactor interface/controller datasheet. *Tactor interface/controller datasheet.* [Online] http://www.eaiinfo.com.

61. **Arduino.** Arduino Mega datasheet. *Arduino.* [Online] http://arduino.cc/en/Main/ArduinoBoardMega.

62. AVR Solutions. *ATmega1280 datasheet.* [Online] http://www.atmel.com/dyn/products/product_card.asp?part_id=3633.

63. **Corporation, Burr-Brown.** OPA547 Datasheet. [Online]

64. **semiconductor, Farchild.** CD4066BC Datasheet. [Online] http://www.fairchildsemi.com.

65. **Enginnering Acoustics, INC.** www.eaiinfo.com. *C2 Tactor Datasheet.* [Online] 2008.

66. *Mechanical properties and Young's modulus of human skin in vivo.* **Agache, P.G., Monneur, C., Leveque, J.L., De Rigal, J.** 3, France : Archives of Dermatological Research, 1980, Vol. 269.

67. *On the relation between indentation hardness and Young's modulus.* **Gent, A. N.** 1958, International Rubber Institute Transactions, Vol. 34, pp. 46–57.

68. **Giang, W., Masnavi, E., Burns, C., Aghaei, B., Morita, P.P., Rizvi, R., Bodjadla, A.** *Baseline and Multimodal GCS Interface Design.* Toronto : Defence R&D Canada, 2011.

69. **McKinely, R.A., Gallimore, J., Lanning, C., Simmons, C., (Report No AFRL-HE-WP-TP-2005-0009).** *Tactile Cueing for Target Acquisition and Identification.* Dayton, Ohio : Human Factors Engineering Department of Wright State University, 2005.

70. *The differential effect of vibrotactile and auditory cues on visual spatial attention.* **Ho, C., Tan H. Z., Spence, C.** 2006, Ergonomics, Vol. 49, pp. 724-738.

71. The CyberTouch glove developed by Immersion Corporation. [Online] Immersion Corporation. http://www.immersion.com.

72. *Cross-modal links in attention between audition, vision and touch: Implications for interface design.* **Spence, C., Driver, J.** 1997, International Journal of Cognitive Ergonomics, Vol. 1, pp. 351-373.

73. *Multimodal threat cueing in simulated combat vehicle.* **Oskarsson, P., Eriksson, L., Lif, P., Lindahl, B., & Hedström, J.** Santa Monica : Human Factors and Ergonomics Society, 2008. In Proceedings of the 52nd Annual Meeting of the Human Factors and Ergonomics Society. pp. 1287-1291.

74. **Donmez, B., Graham, H., & Cummings, M.** *Assessing the Impact of Haptic Peripheral Displays for UAV Operators.* Cambridge : MA: MIT Humans and Automation Laboratory, 2008. Retrieved from http://www.dtic.mil/cgi-bin/GetTRDoc?AD=ADA479798&Location=U2&doc=GetTRDoc.pdf . Report No. HAL2008-02.

75. *Evaluation of tactile alerts for control station operation.* **Calhoun, G., Draper, M., Ruff, H., Fontejon, J., & Guilfoos, B.** Santa Monica, CA : Human Factors and Ergonomics Society, 2003. In Proceedings of the 47th Annual Meeting of the Human Factors and Ergonomics Society. pp. 2118-2122.

76. *Tactile versus aural redundant alert cues for UAV control applications.* **Calhoun, G., Fontejon, J., Draper, M., Ruff, H., & Guilfoos, B.** Santa Monica, CA : Human Factors and Ergonomics Society, 2004. In Proceedings of the 48th Annual Meeting of the Human Factors and Ergonomics Society. pp. 137-141.

77. **Van Erp, J.B.F., Self, B.P.** *Tactile Displays for Orientation, Navigation and Communication in Air, Sea and Land Environments.* s.l. : North Atlantic Treaty Organization, Research and Technology Organization publication, 2008.

78. [Online] Engineering Acoustics Inc. http://www.eaiinfo.com.

79. *Vibrotactile spatial acuity on the torso: effects of location and timing parameters.* **Van Erp, J. B. F.** 2005. Proceedings of the First Joint Eurohaptics Conference and Symposium on Haptic Interfaces for Virtual Environment and Teleoperator Systems. pp. 80-85.

80. *Presenting directions with a vibrotactile torso Display.* **Van Erp, J. B. F.** 2005, Ergonomics, Vol. 48, pp. 302 -313.

81. **Craig, J.C.** 1972, Perception and Psychophysics, Vol. 11(2), pp. 150-152.

82. **Cholewaik, R. W., Collins, A. A., Brill, C. J.** Spatial Factors in Vibrotactile Pattern Perception.

Appendix A

The C2 Tactor Datasheet

The C-2 Tactor† is a miniature vibrotactile transducer that has been optimized to create a strong, localized sensation on the body. Using a body-referenced arrangement of Tactors activated individually, sequentially or in groups, C-2 Tactors can provide intuitive "tactile" instruction to a user. EAI's C-2 Tactor represents a state-of-the-art, wearable vibrotactile transducer, suitable for a wide variety of military, biomedical and commercial applications.

C-2 Tactor, actual size

†patent pending

SPECIFICATIONS: C-2 TACTOR

Physical Description:	1.2" diameter by 0.31" high
Weight:	17 grams
Exposed Material:	anodized aluminum, polyurethane
Electrical Wiring:	Flexible, insulated, #24 AWG.
Skin Contactor:	0.3" diameter, pre-loaded on skin.
Electrical Characteristics:	7.0 ohms nominal.
Insulation Resistance:	50 megohm minimum at 25 Vdc, leads to housing.
Response Time:	33 ms max
Transducer Linearity:	+/- 1 dB from sensory threshold to 0.04" peak displacement.
Recommended Drive:	Sine wave tone bursts 250Hz at 0.25A rms nominal, 0.5 A rms max for short durations.
Recommended Driver:	Bipolar, linear or switching amplifier, 1 W max, 0.5 W typical.

DETAILS OF OPERATION

The C-2 Tactor is a linear actuator that has been optimized for use against the skin. The C-2 Tactor incorporates a moving "contactor" that is lightly preloaded against the skin. When an electrical signal is applied, the "contactor" oscillates perpendicular to the skin, while the surrounding skin area is "shielded" with a passive housing. Thus, unlike most vibrational transducers (such as common eccentric mass motors that simply shake the entire device), the C-2 provides a strong, point-like sensation that is easily felt and localized.

For optimum vibrotactile efficiency, the C-2 is designed with a primary resonance in the 200-300 Hz range that coincides with peak sensitivity of the Pacinian corpuscle, the skin's mechanoreceptors that sense vibration. The C-2's high force and displacement level allow the vibration to be easily felt at all locations on the body, even through layers of clothing.

EAI's offers Tactors in various configurations for different applications – please contact us for details. EAI also offers multi-channel controller/interface boards and complete turnkey vibrotactile systems.

INFORMATION through the sense of TOUCH

From left: C-2 Tactor with Silicone Gel "snap-in" mounting pad; C-2 Tactor with integral polyurethane flange for sewing into a garment; ruggedized C2-A Tactor with internal moisture/sand seal and highly flexible "tinsel" wire with Kevlar strength member.

ENGINEERING ACOUSTICS, INC.

Appendix B

PCB PIEZOTRONICS Vibration Sensor Datasheet

PCB PIEZOTRONICS

Model 352C22

Product Type: Accelerometer, Vibration Sensor

Miniature, lightweight (0.5 gm), ceramic shear ICP® accel., 10 mV/g, 1 to 10k Hz, 10-ft detachable, side exit cable

PERFORMANCE	ENGLISH	SI	
Sensitivity (± 15 %)	10 mV/g	1.0 mV/(m/s^2)	
Measurement Range	± 500 g pk	± 4900 m/s^2 pk	
Frequency Range (± 5 %)	1.0 to 10,000 Hz	1.0 to 10,000 Hz	
(± 10 %)	0.7 to 13,000 Hz	0.7 to 13,000 Hz	
(± 3 dB)	0.3 to 20,000 Hz	0.3 to 20,000 Hz	
Resonant Frequency	≥ 50 kHz	≥ 50 kHz	
Broadband Resolution (1 to 10,000 Hz)	0.002 g rms	0.02 m/s^2 rms	[1]
Non-Linearity	≤ 1 %	≤ 1 %	[2]
Transverse Sensitivity	≤ 5 %	≤ 5 %	
ENVIRONMENTAL			
Overload Limit (Shock)	± 10,000 g pk	± 98,000 m/s^2 pk	
Temperature Range (Operating)	-65 to +250 °F	-54 to +121 °C	
Temperature Response	See Graph	See Graph	
ELECTRICAL			
Excitation Voltage	18 to 30 VDC	18 to 30 VDC	
Constant Current Excitation	2 to 20 mA	2 to 20 mA	
Output Impedance	≤ 300 ohm	≤ 300 ohm	
Output Bias Voltage	7 to 11 VDC	7 to 11 VDC	
Discharge Time Constant	1.0 to 3.5 sec	1.0 to 3.5 sec	
Settling Time (within 10% of bias)	<3 sec	<3 sec	
Spectral Noise (1 Hz)	800 µg/√Hz	7840 (µm/s^2)/√Hz	[1]
(10 Hz)	250 µg/√Hz	2450 (µm/s^2)/√Hz	[1]
(100 Hz)	60 µg/√Hz	590 (µm/s^2)/√Hz	[1]
(1 kHz)	20 µg/√Hz	196 (µm/s^2)/√Hz	[1]
(10 kHz)	10 µg/√Hz	98 (µm/s^2)/√Hz	[1]
Electrical Isolation (Base)	>10^8 ohm	>10^8 ohm	
PHYSICAL			

Appendix C

The Arduino board C code

```c
#include <avr/io.h>
#include <avr/pgmspace.h>
#include <avr/interrupt.h>
#include <math.h>


// COMMON VARIABLE DEFINITION
//--------------------------
byte WaveData_Sine[256], WaveData_Triangle[256], WaveData_Saw[256],
WaveData_Square[256], WaveData_Off[256];                          //
Arrays for holding different look-up table information
byte WaveData_PORTA[256], WaveData_PORTC[256], WaveData_PORTF[256],
WaveData_PORTK[256], WaveData_PORTL[256] ;                        //
Arrays for holding PORT look-up tables
unsigned long int tuningWordMA, tuningWordMC, tuningWordMF,
tuningWordMK, tuningWordML;
// Variables for holding Tuning Word values
int upperCountingValue = 255, desiredfreqA, desiredfreqC,
desiredfreqF, desiredfreqK, desiredfreqL;
// Upper counting value and variables for holding desired frequencies
for different ports
double refFrequency;
// Refrence Frequncy
long int
phaseAccumulatorA,phaseAccumulatorC,phaseAccumulatorF,phaseAccumulator
K,phaseAccumulatorL;                                             // Variables
for holding Phase Accumulator values

void GenerateWaveData_Sine();                            // This
function generates Sinewave look-up table
void GenerateWaveData_Triangle();                       // This
function generates Triangle-wave look-up table
void GenerateWaveData_Saw();                            // This
function generates Sawtooth-wave look-up table
void GenerateWaveData_Square();                         // This
function generates Square-wave look-up table
void GenerateWaveData_Off();                            // Turn
function turns off the port


void setup()
{
  // MICROCONTROLLER REGISTER SETUP
  //------------------------------
```

```
  int k=0;
  cli();                          // Disable interrupts while setting
registers
  TCCR1A = 0;                     // Reset control registers
  TCCR1B = 0;                     // Reset control registers
  TCCR1B |= (1 << WGM12);         // Clear Timer on Compare Match (CTC)
Mode
  TCCR1B |= (1 << CS10);          // Prescaler x1
  OCR1A = 1023;                   // Set compared value
  TIMSK1 = 0;                     // Reset Timer/Counter1 Interrupt Mask
Register
  TIMSK1 |= (1 << OCIE1A);        // Enable Output Compare Match A
Interrupt

  Serial.begin(38400);        // Open serial port, sets data rate to
9600 bps
//  Serial.println("Insert [Port name|Wave form|Gain|Desired
frequency]");

  DDRA = B11111111;               // Set PORTA as output
  DDRB = B11111111;               // Set PORTB as output
  DDRC = B11111111;               // Set PORTC as output
  DDRD = B11111111;               // Set PORTC as output
  DDRF = B11111111;               // Set PORTF as output
  DDRG = B11111111;               // Set PORTC as output
  DDRJ = B11111111;               // Set PORTJ as output
  DDRK = B11111111;               // Set PORTK as output
  DDRL = B11111111;               // Set PORTL as output


  //GENERATE REQUIRED DATA
  //----------------------
  GenerateWaveData_Sine();        // Generate Sinewave look-up table
  GenerateWaveData_Triangle();    // Generate Triangle-wave look-up
table
  GenerateWaveData_Saw();         // Generate Sawtooth-wave look-up
table
  GenerateWaveData_Square();      // Generate Square-wave look-up
table
  GenerateWaveData_Off();         // Turn off the port

  bitSet(PORTD,7);
  bitSet(PORTB,3);
  bitSet(PORTB,7);
  bitSet(PORTD,3);
  bitSet(PORTJ,1);
```

```
  for(k=0; k<256; k++)                         //Turn off all of the
ports when the system start working
  {
    WaveData_PORTA[k]=WaveData_Off[k];
    WaveData_PORTC[k]=WaveData_Off[k];
    WaveData_PORTF[k]=WaveData_Off[k];
    WaveData_PORTK[k]=WaveData_Off[k];
    WaveData_PORTL[k]=WaveData_Off[k];
  }

  //Default setting
  //---------------
  desiredfreqA=1000;
  desiredfreqC=1000;
  desiredfreqF=1000;
  desiredfreqK=1000;
  desiredfreqL=1000;

  refFrequency = 16000000/(upperCountingValue+1);
  tuningWordMA = ((pow(2, 32) * desiredfreqA) / refFrequency);
  tuningWordMC = ((pow(2, 32) * desiredfreqC) / refFrequency);
  tuningWordMF = ((pow(2, 32) * desiredfreqF) / refFrequency);
  tuningWordMK = ((pow(2, 32) * desiredfreqK) / refFrequency);
  tuningWordML = ((pow(2, 32) * desiredfreqL) / refFrequency);

  sei();
}


void loop()
{
  char SERIAL_buffer[5], PORT_buffer, WAVE_buffer, GAIN_buffer,
FREQ_buffer[3];
  int i=0 , j=0, k=0, FREQ;

  if (Serial.available() > 0)
  {

    while (i < 6)
    {

      if (Serial.available() > 0)
      {
      SERIAL_buffer[i]=Serial.read();
      i++;
      }
      delayMicroseconds(1000);
      //delay(1);
```

```
  }

 Serial.println(SERIAL_buffer);

 PORT_buffer = SERIAL_buffer[0];
// Serial.println(PORT_buffer);

 WAVE_buffer = SERIAL_buffer[1];
// Serial.println(WAVE_buffer);

 GAIN_buffer = SERIAL_buffer[2];
// Serial.println(GAIN_buffer);

 for (j=0; j<3 ; j++)
 {
   FREQ_buffer[j]=SERIAL_buffer[j+3];
 }

 FREQ= atoi(FREQ_buffer);
// Serial.println(FREQ);

 switch(PORT_buffer){

 case'A':
   desiredfreqA = 4*FREQ;
   tuningWordMA = ((pow(2, 32) * desiredfreqA) / refFrequency);

   switch(WAVE_buffer){

   case'a':
     for(k=0; k<256; k++)
       WaveData_PORTA[k]=WaveData_Sine[k];
     break;

   case'b':
     for(k=0; k<256; k++)
       WaveData_PORTA[k]=WaveData_Triangle[k];
     break;

   case'c':
     for(k=0; k<256; k++)
       WaveData_PORTA[k]=WaveData_Saw[k];
     break;

   case'd':
     for(k=0; k<256; k++)
       WaveData_PORTA[k]=WaveData_Square[k];
     break;
```

```
      case'e':
        for(k=0; k<256; k++)
          WaveData_PORTA[k]=WaveData_Off[k];
        break;
      }

      switch(GAIN_buffer){
            case'1':
                bitSet(PORTD,7);
                bitClear(PORTG,2);
                bitClear(PORTG,1);
                bitClear(PORTG,0);
            break;

            case'2':
                bitSet(PORTG,2);
                bitClear(PORTD,7);
                bitClear(PORTG,1);
                bitClear(PORTG,0);
            break;

            case'3':
                bitSet(PORTG,1);
                bitClear(PORTD,7);
                bitClear(PORTG,2);
                bitClear(PORTG,0);
            break;

            case'4':
                bitSet(PORTG,0);
                bitClear(PORTD,7);
                bitClear(PORTG,2);
                bitClear(PORTG,1);
            break;
      }

      break;

    case'C':
      desiredfreqC = 4*FREQ;
      tuningWordMC = ((pow(2, 32) * desiredfreqC) / refFrequency);

      switch(WAVE_buffer){
      case'a':
        for(k=0; k<256; k++)
          WaveData_PORTC[k]=WaveData_Sine[k];
        break;
```

```
case'b':
  for(k=0; k<256; k++)
    WaveData_PORTC[k]=WaveData_Triangle[k];
  break;

case'c':
  for(k=0; k<256; k++)
    WaveData_PORTC[k]=WaveData_Saw[k];
  break;

case'd':
  for(k=0; k<256; k++)
    WaveData_PORTC[k]=WaveData_Square[k];
  break;

case'e':
  for(k=0; k<256; k++)
    WaveData_PORTC[k]=WaveData_Off[k];
  break;
}

switch(GAIN_buffer){
      case'1':
          bitSet(PORTB,3);
          bitClear(PORTB,2);
          bitClear(PORTB,1);
          bitClear(PORTB,0);
      break;

      case'2':
          bitSet(PORTB,2);
          bitClear(PORTB,3);
          bitClear(PORTB,1);
          bitClear(PORTB,0);
      break;

      case'3':
          bitSet(PORTB,1);
          bitClear(PORTB,3);
          bitClear(PORTB,2);
          bitClear(PORTB,0);
      break;

      case'4':
          bitSet(PORTB,0);
          bitClear(PORTB,3);
          bitClear(PORTB,2);
```

```
                bitClear(PORTB,1);
            break;
    }

    break;

case'F':
    desiredfreqF=4*FREQ;
    tuningWordMF = ((pow(2, 32) * desiredfreqF) / refFrequency);

    switch(WAVE_buffer){
    case'a':
        for(k=0; k<256; k++)
            WaveData_PORTF[k]=WaveData_Sine[k];
        break;

    case'b':
        for(k=0; k<256; k++)
            WaveData_PORTF[k]=WaveData_Triangle[k];
        break;

    case'c':
        for(k=0; k<256; k++)
            WaveData_PORTF[k]=WaveData_Saw[k];
        break;

    case'd':
        for(k=0; k<256; k++)
            WaveData_PORTF[k]=WaveData_Square[k];
        break;

    case'e':
        for(k=0; k<256; k++)
            WaveData_PORTF[k]=WaveData_Off[k];
        break;
    }

    switch(GAIN_buffer){
            case'1':
                bitSet(PORTB,7);
                bitClear(PORTB,6);
                bitClear(PORTB,5);
                bitClear(PORTB,4);
            break;

            case'2':
                bitSet(PORTB,6);
                bitClear(PORTB,7);
```

78

```
                bitClear(PORTB,5);
                bitClear(PORTB,4);
            break;

            case'3':
                bitSet(PORTB,5);
                bitClear(PORTB,7);
                bitClear(PORTB,6);
                bitClear(PORTB,4);
            break;

            case'4':
                bitSet(PORTB,4);
                bitClear(PORTB,7);
                bitClear(PORTB,6);
                bitClear(PORTB,5);
            break;
    }

    break;

case'K':
    desiredfreqK=4*FREQ;
    tuningWordMK = ((pow(2, 32) * desiredfreqK) / refFrequency);

    switch(WAVE_buffer){
    case'a':
        for(k=0; k<256; k++)
            WaveData_PORTK[k]=WaveData_Sine[k];
        break;

    case'b':
        for(k=0; k<256; k++)
            WaveData_PORTK[k]=WaveData_Triangle[k];
        break;

    case'c':
        for(k=0; k<256; k++)
            WaveData_PORTK[k]=WaveData_Saw[k];
        break;

    case'd':
        for(k=0; k<256; k++)
            WaveData_PORTK[k]=WaveData_Square[k];
        break;

    case'e':
        for(k=0; k<256; k++)
```

```
              WaveData_PORTK[k]=WaveData_Off[k];
         break;
      }

   switch(GAIN_buffer){
         case'1':
              bitSet(PORTD,3);
              bitClear(PORTD,2);
              bitClear(PORTD,1);
              bitClear(PORTD,0);
         break;

         case'2':
              bitSet(PORTD,2);
              bitClear(PORTD,3);
              bitClear(PORTD,1);
              bitClear(PORTD,0);
         break;

         case'3':
              bitSet(PORTD,1);
              bitClear(PORTD,3);
              bitClear(PORTD,2);
              bitClear(PORTD,0);
         break;

         case'4':
               bitSet(PORTD,0);
               bitClear(PORTD,3);
               bitClear(PORTD,2);
               bitClear(PORTD,1);
         break;
      }

   break;

 case'L':
   desiredfreqL = 4*FREQ;
   tuningWordML = ((pow(2, 32) * desiredfreqL) / refFrequency);

   switch(WAVE_buffer){
   case'a':
     for(k=0; k<256; k++)
       WaveData_PORTL[k]=WaveData_Sine[k];
     break;

   case'b':
     for(k=0; k<256; k++)
```

80

```
          WaveData_PORTL[k]=WaveData_Triangle[k];
      break;

case'c':
    for(k=0; k<256; k++)
        WaveData_PORTL[k]=WaveData_Saw[k];
    break;

case'd':
    for(k=0; k<256; k++)
        WaveData_PORTL[k]=WaveData_Square[k];
    break;

case'e':
    for(k=0; k<256; k++)
        WaveData_PORTL[k]=WaveData_Off[k];
    break;
}

switch(GAIN_buffer){
        case'1':
            bitSet(PORTJ,1);
            bitClear(PORTJ,0);
            bitClear(PORTH,1);
            bitClear(PORTH,0);
        break;

        case'2':
            bitSet(PORTJ,0);
            bitClear(PORTJ,1);
            bitClear(PORTH,1);
            bitClear(PORTH,0);
        break;

        case'3':
             bitSet(PORTH,1);
             bitClear(PORTJ,0);
             bitClear(PORTJ,1);
             bitClear(PORTH,0);
        break;

        case'4':
            bitSet(PORTH,0);
            bitClear(PORTJ,0);
            bitClear(PORTJ,1);
            bitClear(PORTH,1);
        break;
}
```

```
      break;
    }

  // Serial.println("Insert [Port name|Wave form|Gain|Desired
frequency]");
  }
}


//OTHER FUNCTIONS
//--------------

void GenerateWaveData_Sine()
//This function generates Sinewave look-up table
{
  for (int i=0; i < 256; i++)
    WaveData_Sine[i] = (255*(sin((i*6.2831)/256)+1))/2;
}

void GenerateWaveData_Triangle()
//This function generates Triangle-wave look-up table
{
  for (int i=0; i < 128; i++)
    WaveData_Triangle[i] = (i*255*2)/256;
  for (int i=128; i < 256; i++)
    WaveData_Triangle[i] = ((256-i)*255*2)/256;
}

void GenerateWaveData_Saw()
//This function generates Sawtooth-wave look-up table
{
  for (int i=0; i < 256; i++)
    WaveData_Saw[i]=i;
}

void GenerateWaveData_Square()
//This function generates Square-wave look-up table
{
  for (int i=0; i < 256/2; i++)
    WaveData_Square[i] = 0;
  for (int i=256/2; i < 256; i++)
    WaveData_Square[i] = 255;
}

void GenerateWaveData_Off()
{
  for (int i=0; i < 256; i++)
    WaveData_Off[i] = 0;
```

```
}

//INTERRUPTS
//----------
ISR(TIMER1_COMPA_vect)                                    //
Interrupt service run when Timer/Counter1 reaches OCR1A
{

  phaseAccumulatorA += tuningWordMA;
  phaseAccumulatorC += tuningWordMC;
  phaseAccumulatorF += tuningWordMF;
  phaseAccumulatorK += tuningWordMK;
  phaseAccumulatorL += tuningWordML;

  byte phaseAccumulatorMSBA = (phaseAccumulatorA >> 24);
  byte phaseAccumulatorMSBC = (phaseAccumulatorC >> 24);
  byte phaseAccumulatorMSBF = (phaseAccumulatorF >> 24);
  byte phaseAccumulatorMSBK = (phaseAccumulatorK >> 24);
  byte phaseAccumulatorMSBL = (phaseAccumulatorL >> 24);

  PORTA = WaveData_PORTA[phaseAccumulatorMSBA];
  PORTC = WaveData_PORTC[phaseAccumulatorMSBC];
  PORTF = WaveData_PORTF[phaseAccumulatorMSBF];
  PORTK = WaveData_PORTK[phaseAccumulatorMSBK];
  PORTL = WaveData_PORTL[phaseAccumulatorMSBL];
}
```